Aviation-Climate Change Research Initiative (ACCRI)

Subject specific white paper (SSWP) on

Contrails/cirrus optics and radiation

SSWP # VI

Dr. Ping Yang, PI
Dr. Andrew Dessler, Co-PI
Dr. Gang Hong, Team member

Department of Atmospheric Sciences
Texas A&M University
College Station, TX 77843

January 22, 2008

Table of Content

Optical properties and radiative forcing of contrails

Ping Yang (PI), Andrew Dessler (Co-PI), and Gang Hong (Team member)

Department of Atmospheric Sciences
Texas A&M University
College Station, Texas 77843-3150

Email: pyang@ariel.met.tamu
adessler@tamu.edu
hong@ariel.met.tamu.edu

January 22, 2007

Executive Summary

The effect of aircraft emissions on the climate of Earth is one of the most serious long-term environmental issues facing the aviation industry (IPCC, 1999; Aviation and the Environment – Report to the United States Congress, 2004). Aviation emissions, including gases and particles in the upper troposphere and lower stratosphere, have both direct and indirect climate effects. The direct effect is principally the emission of carbon dioxide, a powerful greenhouse gas. The indirect effects include the changes in ozone due to emissions in nitrogen oxides, the effects of aerosol emissions and water vapor on clouds, and the effects associated with contrails and contrail-induced cirrus clouds.

As stated in *the Executive Summary of the Workshop on the Impacts of Aviation on Climate Change,* June 7-9, 2006, Boston, MA (hereafter, the *Workshop Executive Summary*, http://web.mit.edu/aeroastro/partner/reports/climatewrksp-rpt-0806.pdf), "The effects of aircraft emissions on the current and projected climate of our planet may be the most serious long-term environmental issue facing the aviation industry… The only way to ensure that policymakers fully understand trade-offs from actions resulting from implementing engine and fuel technological advances, airspace operational management practices, and policy actions imposed by national and international bodies is *to provide them with metrics that correctly capture the climate impacts of aviation emissions.*"

Cloud radiative forcing, defined as the difference of shortwave and longwave radiative fluxes between cloudy and clear-sky conditions, is *a common metric* to quantify the effect of clouds on climate. In addition, the optical properties of cloud particles are fundamental physical quantities that are connected to cloud radiative forcing. Significant uncertainties exist in our present understanding of the radiative forcing and optical properties of contrails and contrail cirrus clouds, as explicitly stated in the *Executive Summary.*

With the support of the Volpe National Transportation System Center under the solicitation "Aviation-Climate Change Research Initiative (ACCRI)" (DTRT57-07-2003), this subject-specific white paper reports on the 5th key area identified in the solicitation, i.e., *Climate Impacts of Contrails and Contrail-Cirrus*. Specifically, this report provides a review of our current knowledge of

(1) the optical properties of individual ice crystals in contrails and contrail-cirrus clouds from modeling and measurement (including laboratory analog measurements) perspectives;
(2) the bulk optical properties of contrails and contrail-cirrus clouds, including the effect of ice crystal size-habit distributions; and
(3) the radiative forcing of contrails and contrail-cirrus cloud systems.

In this report, the current state of science on the climate impacts of contrails and contrail-induced cirrus is reviewed, including an analysis of the uncertainties. In so doing, we identify ten key problems:

- The uncertainties in contrail and contrail-induced cirrus coverage estimated from different detection algorithms and measurements.
- The uncertainties in optical thicknesses of contrail and contrail-induced cirrus clouds from different analyses. These differences result in distinct differences in the radiative forcing of contrails and contrail-induced cirrus clouds.
- Ice particle sizes vary from contrails to contrail-induced cirrus clouds. But the measurements for ice particle sizes are strongly dependent on the detection approaches, particularly for small ice particles.
- Different ice habits have been found in contrails and contrail-induced cirrus clouds. In turn, different mixtures of ice habits must be used in the study of the radiative forcing of contrails and contrail-induced cirrus clouds. A better understanding of the single-scattering properties of ice crystals in contrails and contrail-induced cirrus clouds is necessary.
- Shortwave radiative forcing varies substantially with solar zenith angle. The diurnal variation of air traffic is an important factor for the radiative forcing calculations, but is often neglected in the calculation of the impact of contrails and contrail-induced cirrus.
- New techniques should be developed to accurately detect contrails and contrail-induced cirrus clouds. This is critical for understanding the microphysical and optical properties of these clouds.
- Our current understanding of the effects of aerosols emitted by aircraft on cirrus cloud formation and the interaction between aerosols and cirrus clouds needs to be improved. Furthermore, the chemical effects of black carbon and sulphate particles on the microphysical properties (e.g., the refractive indexes) of ice particles in contrails and contrail-induced cirrus clouds are poorly known and need to be improved.
- There are no studies on the contrails embedded within natural cirrus clouds. This is quite important since the aircraft flight heights are often at the heights where ice clouds frequently occur.

- Representation of contrails and contrail-induced cirrus clouds in global atmospheric models needs to be improved. There are shortages of observations for validation of GCM results, and the representation of the aerosol-cirrus interaction in GCMs needs substantial improvements. Furthermore, there is an urgent need to develop radiation schemes that are suitable for use in GCMs.
- More and better measurements of supersaturation in the atmosphere.

To reduce the above uncertainties in estimating the radiative forcing of contrails and contrail-induced cirrus clouds, we recommend the following prioritized research areas:

- *Area 1*. Development of a database of the single-scattering properties of ice particles and aerosols in contrails and contrail-induced cirrus clouds. Although various habits of ice crystals have been found in contrails and contrail-induced cirrus clouds, there is not a single-scattering database specified for studies involving contrails and contrail-induced cirrus clouds. The particle size distributions for contrails tend to have smaller ice particle sizes in comparison with those for natural cirrus clouds. A contrail single-scattering database would provide the basis for retrieving the microphysical and optical properties of contrails and contrail-induced cirrus clouds and studying their radiative forcing, which could be of great benefit to the community of the scientists who study different aspects of the contrail-ice cloud dependencies.
- *Area 2*. Develop new parameterization schemes for shortwave and longwave radiation calculations in GCMs that are suitable for contrails and contrail-induced cirrus clouds.
- *Area 3*. Improve detection of contrails and contrail-induced cirrus clouds from multiple satellite sensors, including passive radiometric measurements from imagers/interferometers and active lidar and radar sensors. Specifically, we note the availability and maturity of data products from the NASA A-Train suite of satellites. This effort is to provide the microphysical, macrophysical, and optical properties of contrails and contrail-induces cirrus clouds that are essential to the study of the radiative forcing of contrails and contrail-induced cirrus clouds.
- *Area 4*. Make more use of in situ measurements and laboratory experiments to understand the formation of contrails and contrail-induced cirrus clouds, the accurate formation criteria of the formation of contrails, and the physical and chemical processes involved in the transition from contrail to cirrus clouds. Especially, improvement on our knowledge about the effect of water vapor and temperature on contrail formation is a prioritized area.
- *Area 5*. Further use of measurements to improve theoretical models of the interaction between aerosols and cirrus clouds. Global model studies should strive to include both the direct and indirect effects, as well as the effects of the direct and indirect effects on high clouds.

Recommendations for best use of current tools for the prioritized research areas:

A combination of the FDTD (or DDA) method and the geometric optics method (GOM) is recommended for the development of the single-scattering properties of ice

particles and aerosols in contrails and contrail-cirrus clouds. The FDTD and DDA methods are accurate approaches applicable to small particles. The GOM method is an approximation that is valid for large ice crystals. Several studies reported in the literature have shown that this combination of the FDTD and GOM methods is appropriate in the study of the optical properties of nonspherical ice crystals within natural cirrus clouds.

A new parameterization of the bulk radiative properties of contrails and contrail-cirrus clouds is necessary for the radiative transfer schemes used in several popular climate models such as the NCAR Community Atmosphere Model (CAM). The parameterization can be done on the basis of the single-scattering properties of contrails and contrail-induced cirrus clouds, which are derived from the FDTD (or DDA) and GOM. Furthermore, the validation of the parameterization can be carried out by comparing the model simulations of radiation fluxes and measurements (i.e., the CERES data and DOE-ARM ground radiometric measurements).

Existing satellite sensors, including the narrow bands (MODIS, GOES), broad bands (CERES), high-resolution spectra (AIRS), active (CALIPSO), multi-viewing angles (MISR), polarized (POLDER) sensors, provide an unprecedented opportunity to observe contrails and contrail-cirrus clouds. Moreover, the MODIS band 26 centered at 1.375 μm is effective for detecting thin and high clouds including contrails. We recommend to synergistically use the existing satellite-based retrieval products to quantify the extent of contrails and contrail-cirrus clouds from a global perspective.

To improve the current understanding of the formation of contrails and contrail-cirrus clouds, more in-situ observations regarding the relationship between contrails and ambient parameters are recommended. The prediction of water vapor supersaturation has recently been incorporated into some European models such as the ECWMF, ECHAM4, and IFSHAM models. Modeling efforts are also recommended to understand the influence of water vapor and temperature on contrail formation. Furthermore, in situ measurements can be used to validate and improve the representation of supersaturation in models.

The interaction between aerosols and contrail/cirrus clouds is still an open area. More in-situ measurements and laboratory experiments regarding the correlation of aerosols and contrails are recommended. Furthermore, modeling on the basis of cloud resolving models including the interaction of aerosols and contrail/cirrus clouds may also provide an efficient way to study the interaction between aerosols and contrail/cirrus clouds, which is complementary to the recommended in-situ measurements and laboratory experiments.

The costs and timeline for the aforementioned five prioritized research areas are estimated as follows:

- *Area 1:* 2 FTE for 3 years
- *Area 2:* 2 FTE for 2.5 years
- *Area 3:* 3 FTE for 3 years
- *Area 4:* 3 FTE for 3 years
- *Area 5:* 4 FTE for 3 years

1. Introduction and Background

The first task of the Aviation-Climate Change Research Initiative (ACCRI) is to survey and document our current understanding of the impact of aviation on climate in seven key areas. One of these areas is the climate impact of contrails and contrail-cirrus clouds (i.e., contrails that occur within widespread cirrus cloud decks). These features, formed in the wakes of aircraft, provide one of the most visible anthropogenic effects in the atmosphere. They are often observed in the skies, especially near airports in the United States and Europe. Generally, contrails are composed of ice particles and are unique because they tend to have narrow widths and linear shapes, at least initially.

A contrail typically has a relatively short lifetime when formed in a subsaturated environment — e.g., descending air of a high pressure system — and unlikely to have a significant perturbation on climate. However, in supersaturated air — e.g., ascending air of a low pressure system — a contrail may be quite persistent, and can quickly (minutes to hours) spread into an extended cirrus deck. Contrails with longer lifetimes and larger horizontal extent may affect both the radiation budget and climate in a manner similar to natural cirrus clouds except that their microphysical properties are different (Gayet et al., 1996).

Cloud radiative forcing, defined as the difference of the radiative fluxes between cloudy and clear sky at the top of the atmosphere, *is a straightforward metric to estimate the effects of specific cloud on climate* (Ramanathan et al., 1989). It is therefore useful to document the current understanding of the radiative forcing of contrails and contrail-cirrus clouds.

Fu and Liou (1993) suggested that contrails have radiative effects similar to cirrus clouds because they are ice clouds. Thus, they may have significant regional climate effects. IPCC (1999) reported a best estimate of approximately 0.02 Wm^{-2} based on the study of Minnis et al. (1999) of the global distribution of contrail radiative forcing. While contrails may have large regional effects, the magnitude of the radiative forcing tends to reduce when averaged globally. Recently, the global radiative effects of contrails have been further studied by using different datasets, models and methods (Marquart et al., 2003; Fichter et al., 2005). These studies estimated the radiative impact due to linearly shaped contrails. Duda et al. (2001) investigated the evolution of solar and longwave radiative forcing in contrail clusters over the continental United States and Hawaii by using the GOES data and suggested that the microphysical properties (e.g., ice particle shape) of contrails may have an important effect on radiative forcing. Moreover, air traffic annually increases by 2-5%, according to Minnis et al. (1999, 2004).

All these studies indicate that the accuracy of contrail radiative forcing depends on the extent, persistence, and microphysical and optical properties (i.e., the optical thickness, ice particle size, and shape distributions) of contrails. In addition, almost all reported studies of contrails radiative forcing are focused on linearly shaped contrails that can be easily discriminated from natural cirrus in satellite images. Not included in these estimates is the influence of diffuse contrails (contrails that had spread over time) or the influence of aircraft emissions on naturally-occurring cirrus.

Ice particles in contrails and contrail-cirrus clouds are nonspherical particles. Goodman et al. (1998) collected samples of contrail ice particles using an impaction

technique. Their results show that the ice habits at a temperature of approximately -61°C included hexagonal plates (75%), columns (20%) and a few triangular plates (<5%). The nonsphericity of these ice particles must be taken into account in the modeling of the radiative properties of contrails and contrail-cirrus clouds because the radiative impact can be quite different for clouds composed of spherical versus nonspherical particles. For example, Liou et al. (2000) demonstrated that the approximation of nonspherical ice particles as "equivalent" ice spheres for the single-scattering and radiative transfer processes can substantially underestimate ice cloud albedo. Moreover, the single-scattering properties associated with realistic ice particle morphologies must be used for a correct interpretation of other bulk optical properties of cirrus clouds. Consequently, it is important that the nonsphericity of ice particles be accurately modeled in the radiative transfer computations involving contrails or contrail-cirrus clouds.

2. Review of current knowledge of the optical properties and radiative forcing of contrails and contrail-induced cirrus clouds

On any given day, clouds cover approximately 70% of the Earth's surface. Of this total, approximately 30% of the cloud cover occurs at high altitudes where the clouds are composed exclusively of ice particles. Substantial effort has been made in the last three decades to understand and determine the fundamental scattering and absorption properties of ice particles in these high altitude clouds. Early research efforts to account for the nonsphericity of ice crystals assumed that these clouds were composed of long circular cylinders. From the late 1970s to the 1990s, the geometric optics method, by means of the ray-tracing technique, was used extensively to investigate the single-scattering properties of relatively simple nonspherical ice particles (e.g., Takano and Liou, 1989a, b; Macke, 1996). Over the past decade, other methods such as the T-matrix method and the finite-difference time domain method have also been applied to the study of the optical properties of nonspherical ice particles (Mishchenko and Sassen, 1998; Yang and Liou, 2006). Laboratory and in situ measurements of the optical properties of nonspherical ice particles were also reported in the literatures (e.g., Gayet et al. 1996; Barkey et al. 2000). The research results from these efforts have been used in various applications in conjunction with the study of cirrus clouds, e.g., the parameterization of the radiative properties of ice clouds for use in climate models. *Given the wealth of recent progress (e.g., field campaigns and scientific publications) in the understanding of the microphysical and optical properties of ice clouds, it is necessary to first provide a condensed survey of the current scientific understanding of the scattering properties of non-spherical particles.*

2.1 Optical properties of ice particles in contrails and contrail-induced cirrus clouds

2.1.1 Size distributions and habits of ice particles in contrails and contrail-induced cirrus clouds

a. Current state of science

In-situ observations have demonstrated that ice crystals within contrails and contrail-induced cirrus have diverse size distributions. As an example, Figure 1 shows a representative selection of ice crystal number distributions to illustrate the contrail evolution. In general, both small and large ice crystals are found in contrails (e.g., Gayet et al., 1996; Sausen et al., 1998; Minnis et al., 1998; Ström and Ohlsson, 1998; Meerkötter et al., 1999; Schröder et al., 2000; Ponater et al., 2002). During the transition of contrails into cirrus clouds, the ice particles become larger and the number of particles decreases (Schröder et al., 2000). Schröder et al. (2000) investigated the microphysical properties of contrails and contrail-induced cirrus from in situ observations performed during more than 15 airborne missions over central Europe. They found that the observed contrails were dominated by high concentrations (> 100 cm^{-3}) of ice crystals with mean diameters in the range of 1-10 μm. Larger ice crystals in the range 10-20 μm with typical concentrations 2-5 cm^{-3} were found in young contrail-induced cirrus, which mostly contain regularly shaped ice crystals.

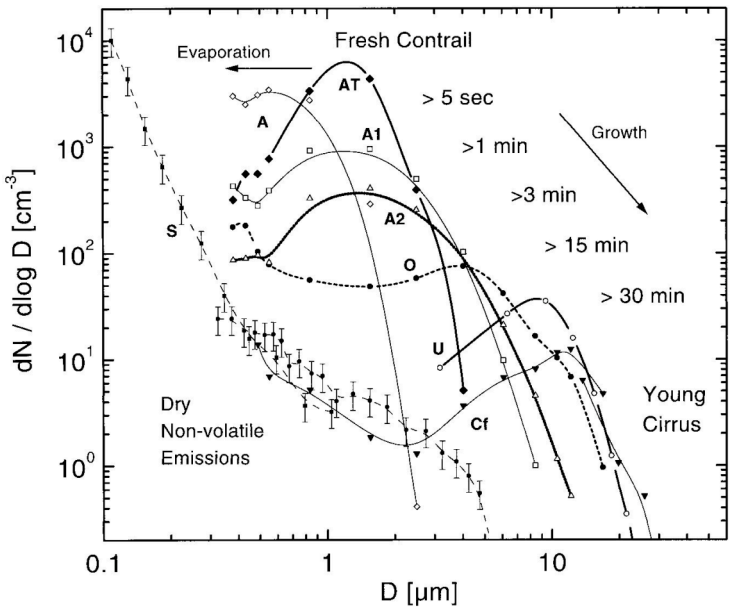

Figure 1. Representative selection of particle concentrations illustrating the transition of contrails into cirrus clouds. AT, A, A1, A2, O, and U are for contrail cases, CF is for young cirrus cloud, and S is for dry exhaust jet aircraft emission. Adapted from Schröder, et al. (2000).

Liou et al. (1998) reported two size distributions measured during the Subsonic Aircraft: Contrail and Cloud Effects Special Study (SUCCESS) on May 4, 1996. In comparison with two size distributions measured by FSSP for a contrail and a cold cirrus on April 18 and 19, 1994, it was shown that the maximum particle sizes in contrails were less than 100 μm. But the typical sizes of ice crystals in natural cirrus clouds range from several tens to hundreds microns.

Large ice crystals in contrails and contrail-induced cirrus are essentially nonspherical, as found from in-situ observations (e.g., Gayet et al., 1996; Sussmann, 1997; Liou et al., 1998; Goodman et al., 1998). Figure 2 shows the examples of scanning microscope images of small crystals (Goodman et al., 1998), including the hexagonal

plates, columns, and triagonal plates. From microphotographs taken from airborne particle sampling in a young contrail (aged 3-4 min) at an altitude between 8 and 9 km and a temperature between –49°C and –53°C, Weickmann (1945, 1949) found a few large (~100 μm) hollow prisms typical of highly ice-supersaturated conditions. Strauss (1994) reported that the ice crystals in a young contrail had a droxtal habit (see Figure 10) with sizes ranging from 1 to 5 μm. These observations were made with an ice replicator instrument. Sussmann (1997) presented photographs of a 120° parhelion and a 22° parhelion within persistent contrails. It was found that the contrails consisted of a considerable number of hexagonal plates orientated horizontally and with diameters between 300 and 2000 μm. This confirms that a subset of the particle population in persistent contrails may be composed of oriented plates and columns that grow at least as regularly as the most regular crystals found in natural cirrus. Immler and Schrems (2003) found that the southern hemispheric cirrus clouds tend to have larger particles than the northern hemispheric cirrus clouds. Furthermore, the southern hemispheric cirrus clouds have higher density of column-like particles whereas the northern hemispheric cirrus clouds seem to be dominated by plates, as found from lidar measurements. This probably reveals that the influence of human activities on the formation of cirrus clouds, which include the aviation emissions that are more intense over the northern hemisphere than over the southern hemisphere.

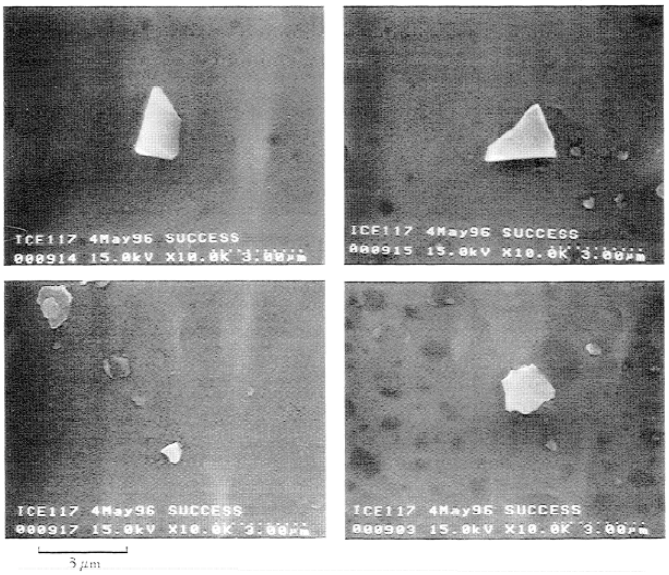

Figure 2. Scanning microscope images of small crystals (Goodmann et al., 1998).

b. Critical role of size distributions and habits of ice crystals

The particle size distribution and habit distribution are two microphysical parameters that are most important to the determination of the bulk optical properties of contrails or contrail-induced cirrus clouds. From the SUCCESS replicator data, Liou et al. (1998) showed that the habits of ice crystals within contrails are approximately 50% bullet rosettes, 30% hollow columns, and 20% plates. They also calculated the bulk single-scattering properties of contrails and cold cirrus shown in Fig. 3. The effective size (Foot, 1988) for a given size distribution is defined as follows:

$$D_e = \frac{3}{2}\frac{\int_{D_1}^{D_2} Vn(D)dD}{\int_{D_1}^{D_2} An(D)dD}, \tag{1}$$

where V and A are the volume and projected area of an ice crystal with a maximum dimension of D, respectively. The quantity n indicates the size distribution. The lower and upper limits of ice crystal sizes are D_1 and D_2, respectively. Note that effective size defined in Eq. (1) is different from that in Liou et al. (1998) by a factor of 3/2. The definition given by Eq. (1) is consistent with that used by the Moderate Resolution Imaging Spectroradiometer (MODIS) operational cloud products (King et al. 2004). Figure 3 shows the asymmetry factor, single-scattering albedo, and extinction coefficient for four ice clouds (Liou et al., 1998). It is evident from Fig. 3 that the bulk optical properties of ice crystals are quite sensitive to the effective size. Note that the differences in the extinction coefficient are caused by the differences in both the effective particle size and total number concentration of ice crystals.

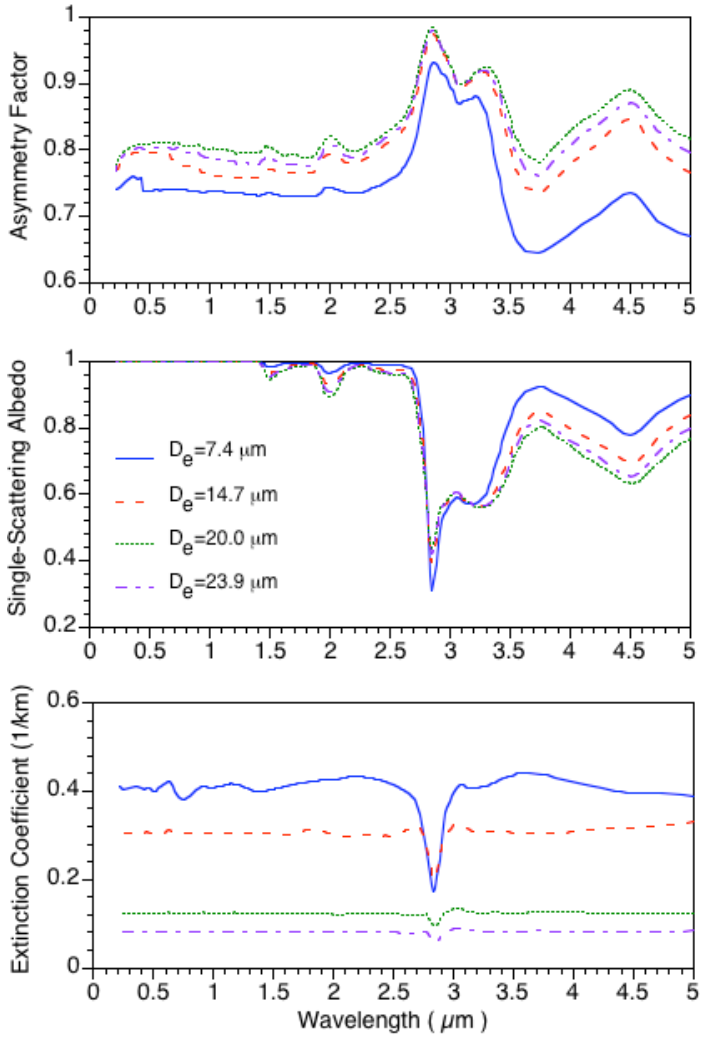

Figure 3. Asymmetry factor, single-scattering albedo, and extinction coefficient as functions of wavelength from 0.2 to 5 μm. The minima located at 2.85 μm are the well-known Christiansen effect. Adapted from Liou et al. (1998). The values of the effective sizes shown in the figure have been converted to the definition given by Eq. (1).

Goodman et al. (1998) collected ice crystal samples in the contrail using an impaction technique. Their results show that the crystal habits at a temperature of -61°C included hexagonal plates (75%), columns (20%) and a few triagonal plates (<5%). The scattering properties of the ice crystals in contrails and natural cirrus are different and result in differences in their radiative forcing. Figure 4 illustrates the effect of ice particle sizes and habits of contrails, contrail-induced cirrus, and natural cirrus on the solar and infrared radiation. The influences of particle effective size and habit on radiation are stronger for solar radiation than for infrared radiation, particularly for thicker cirrus clouds. Furthermore, the influences of particle effective size and habit on infrared radiation are observed primarily for thin cirrus clouds

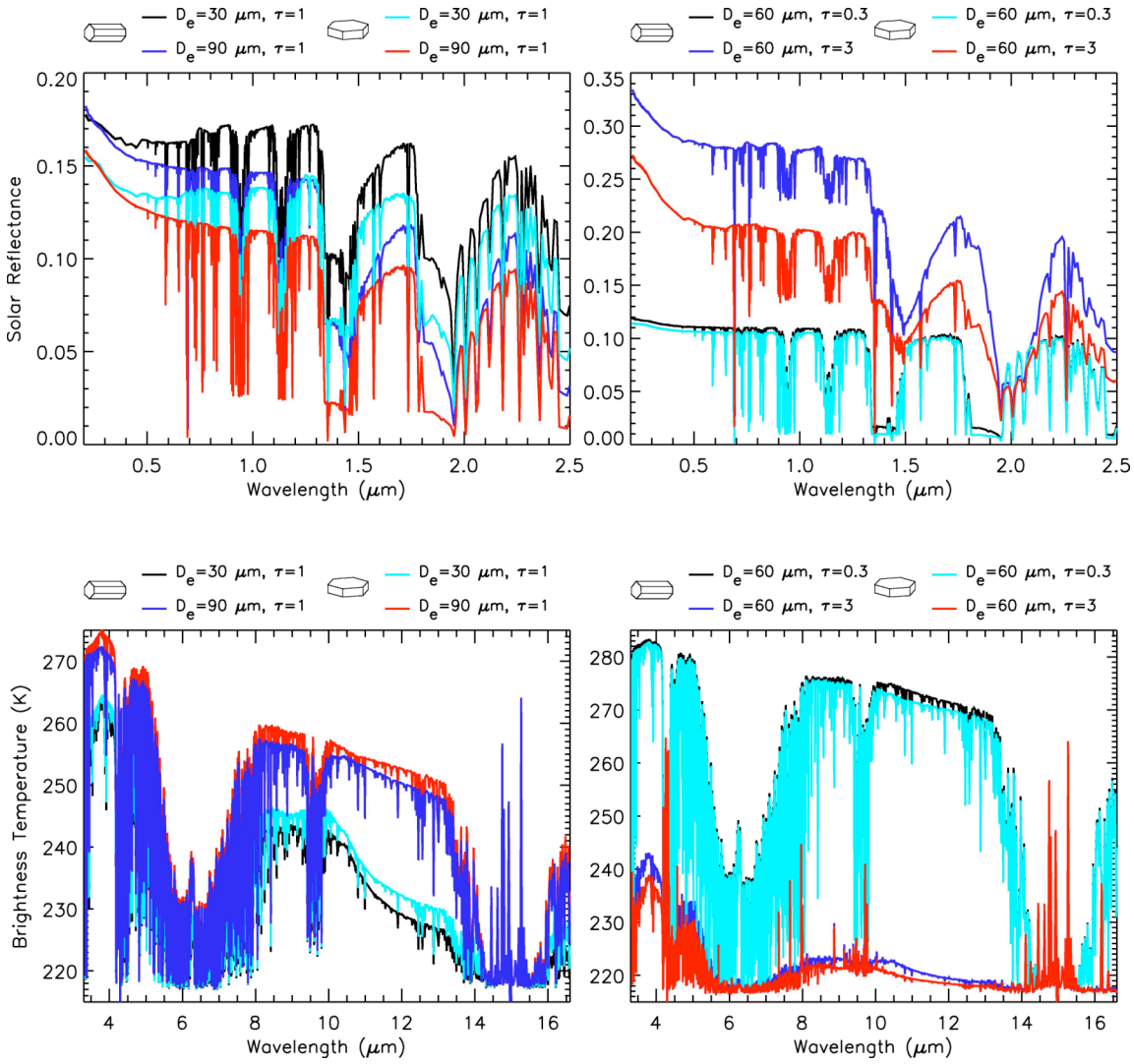

Figure 4. Effects of shape, ice particle size, and optical thickness on solar reflectance spectra (upper panels) and infrared brightness temperature spectra (bottom panels) (Hong et al., unpublished).

2.1.2 Measurements and Simulations of the optical properties of ice crystals

a. Current state of science

As discussed above, the microphysical and optical properties of nonspherical ice crystals are important to the understanding of the radiative impact of contrails. Figs. 5 and 6, adapted from Liou et al. (2000), illustrate the importance of the ice particle nonsphericity in the case of cirrus clouds. It is expected that the nonsphericity of ice

crystals would be important as well in the case of contrails and contrail-induced cirrus clouds. Specifically, Fig. 5 shows the cirrus albedo for the solar spectrum, calculated by assuming particles are plates/columns or spheres, in comparison with measurements from the FIRE field campaign held in Wisconsin during 1986. The shaded area indicates the range of the results corresponding to equivalent spheres. It is evident that neglecting the nonsphericity can lead to significant errors in the radiative effect of cirrus clouds.

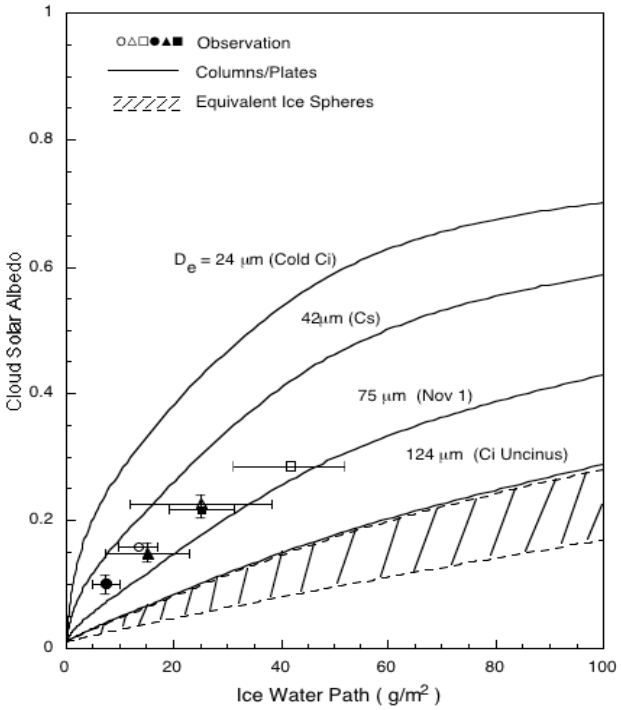

Fig. 5. Solar albedo as a function of ice water path determined from broadband flux observations from aircraft for cirrus clouds that occurred during the FIRE experiment, Wisconsin, November-December, 1986 (Stackhouse and Stephens 1991). The solid lines represent theoretical results computed from a line-by-line equivalent solar model using observed ice crystal sizes and shapes for a range of mean effective ice crystal sizes. The dashed lines are corresponding results for equivalent spheres. Adapted from Liou et al. (2000)

Figure 6 shows the sensitivity of surface temperature to high cloud coverage or the ice water path associated with these clouds based on a 1D cloud and climate model (Liou et al. 2000). For present climate conditions, the simulations based on "equivalent spheres" for nonspherical ice crystals lead to a 0.4-K overestimation of the surface temperature. Thus, the nonsphericity of ice crystals is significant for climate studies.

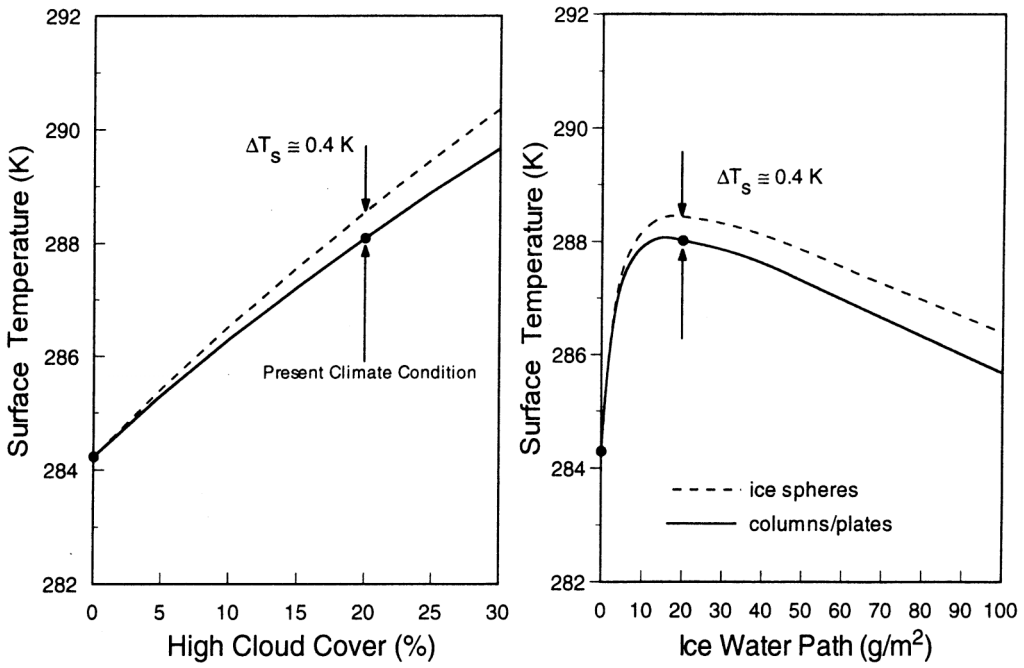

Fig. 6. Surface temperatures determined from a one-dimensional cloud and climate model using a radiative transfer parameterization based on the scattering and absorption properties of hexagonal columns/plates and equivalent ice spheres. The model has a present climate condition corresponding to a surface temperature of 288K involving a typical cirrostratus located at 9 km with a geometric thickness of 1.7 km, an ice water content of 10^{-2} g m^{-3}, and 20% fractional coverage. Perturbations are performed for both cloud cover and IWP. Adapted from Liou et al. (2000).

Laboratory measurements of the optical properties of nonspherical ice crystals generated in cloud chambers have been reported (Sassen and Liou, 1979a,b; Barkey et al. 2000). Gayet et al. (1998) measured the scattering phase functions associated with contrails and natural cirrus and compared the measurements with theoretical calculations. They concluded that, "in contrails and natural cirrus, measured scattering phase function indicates major difference with those used in cloud models which assume ice spheres or simple geometric shape of ice crystals." The scattering properties of individual ice crystals have been measured by Bacon et al. (1998) and Bacon and Swanson (2000). Although laboratory measurements of the optical properties of ice crystals provide very useful information, they are limited in terms of spectral coverage, angular range (necessary for measurements of the scattering phase function), and an incomplete set of the single-scattering properties (i.e., the phase function, extinction cross sections, and single-scattering albedo are not simultaneously measured). Thus, for many practical applications (e.g., the parameterization of the bulk radiative of ice clouds for applications to climate models), a theoretical approach is generally used to infer the single-scattering properties for a wide variety of ice habits.

At present, four numerical methods are usually applied to the computation of the optical properties of nonspherical ice crystals: the geometric optics method (the so-called ray-tracing technique), the T-matrix method, the finite-difference time domain (FDTD) method, and discrete dipole approximation (DDA) method.

The early applications of the principles of geometric optics to the scattering of light by nonspherical ice crystals can be traced back to the studies of Jacobowitz (1971) and Wendling et al. (1979) for 2D and 3D hexagonal ice crystals, respectively. In 1980s and 1990s, the ray-tracing technique was used extensively to compute the optical properties of nonspherical ice crystals with various shapes (Cai and Liou, 1982; Takano and Jayaweera, 1985; Takano and Liou, 1989a,b; Macke, 1993; Hess and Wiegner, 1994; Macke et al., 1993, 1996, Yang and Liou, 1998). Modified geometric optics methods have also been developed (Muinonen, 1989; Yang and Liou, 1995, 1996b, and 1997) to overcome some shortcomings in the conventional ray-tracing technique.

Figure 7 illustrates the physical basis of the conventional ray-tracing technique. When the size of an ice crystal is much larger than the incident wavelength, the incident radiation can be thought of as being composed of a bundle of localized waves or rays. Snell's law and the Fresnel formulas can be employed to trace the propagation of the incident ray and calculate the magnitude and phase of the electric field vector associated with the ray. After propagations of all the incident rays are traced, the angular distribution of scattered energy in conjunction with the incident rays can be obtained. Additionally, diffraction phenomenon also contributes to the scattered energy, which can be accounted for in terms of the classical Fraunhifer diffraction theory.

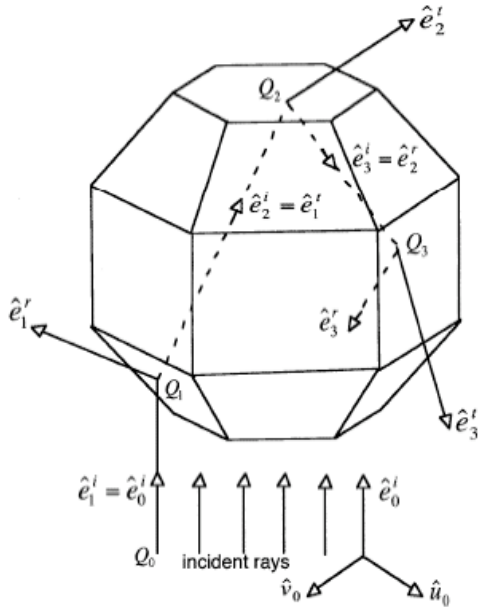

Fig.7. A conceptual diagram for the principle of the ray-tracing technique for computing the single-scattering properties of a particle that is much larger than the incident wavelength. Adapted from Yang and Liou (2006).

The T-matrix method (Waterman 1971, Mishchenko and Travis, 1994) is a computationally efficient method for deriving the optical properties of small and

moderately-sized particles. This method is usually applied to axially symmetric particles (e.g., spheroid and circular cylinders) although this method, in principle, can be applied to an arbitrary particle shape. At present, it is quite challenging to implement the T-matrix method for complex ice crystal shapes such as bullet rosettes and aggregates. The T-matrix method was applied to investigate the depolarization of lidar returns associated with contrails (Mishchenko and Sassen, 1998). The technical details of the method are described in Mishchenko et al. (2000).

The FDTD method pioneered by Yee (1966) is a powerful numerical method to solve electromagnetic scattering problems. In principle, the FDTD method solves Maxwell's equations in the time domain. Fig. 8 illustrates the basic principles of the FDTD method. In the FDTD method, a finite spatial region containing a scattering particle is discretized in terms of a grid mesh and the time-dependent Maxwell curl equations are replaced with their finite-difference analogs. To suppress the artificial reflection due to the truncation of the computational domain, an absorbing boundary condition is applied at the edges of the domain. Then, a plane wave is introduced into the computational domain. The interaction of the incident wave and the scattering particle can be simulated by the finite-difference analogs of the Maxwell equations in the time domain. The signals regarding the interaction between the particle and the incident wave in the time domain can be transformed into their counterparts in the frequency domain. After the near field is obtained in the frequency domain, the near field can be mapped to the far field to derive the single-scattering properties of the particle.

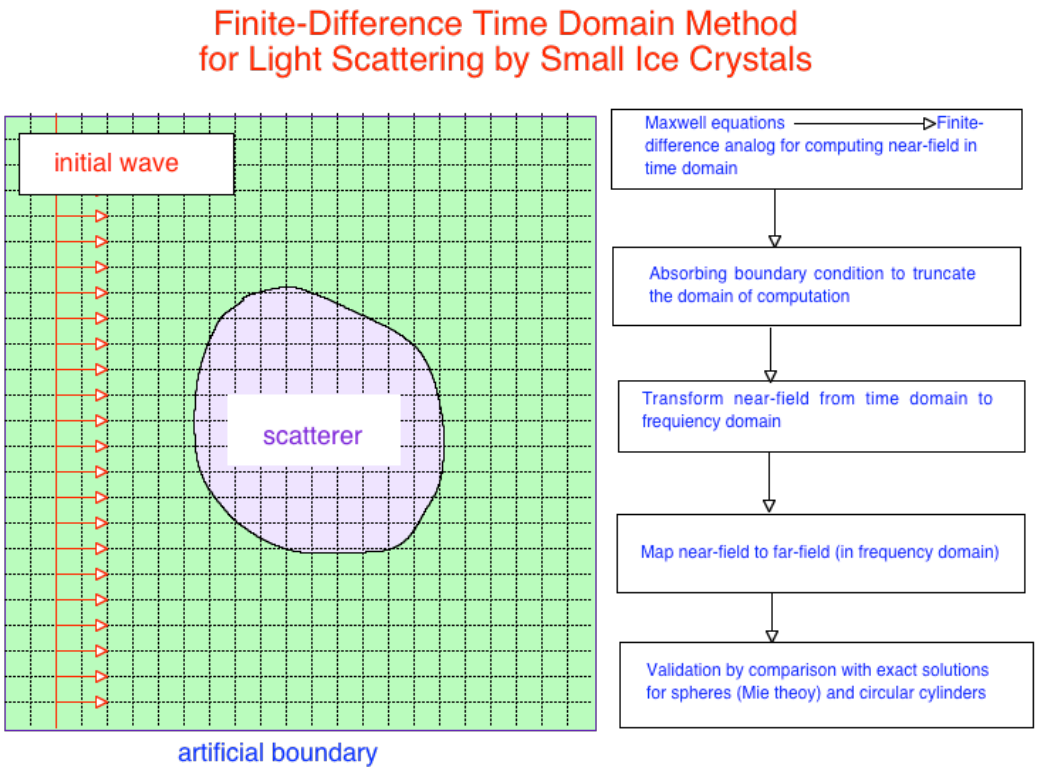

Fig. 8. Schematic diagram illustrating the basic principle of the finite-difference time domain method.

The DDA method was developed originally by Purcell and Pennypacker (1973). In the DDA computation, a scattering particle is approximated by a number of electric dipoles, as shown in Fig. 9. Each dipole responds to local field that is the superposition of the incident field and the field induced by the other dipoles. The governing equations for the coupled dipoles are a set of linear equations. The solutions to the linear equations provide the field scattered by the dipoles, which can be used to compute the optical properties of the scattering particles. A DDA computational code developed by Drain and Flatau (1994) has been released for non-commercial applications.

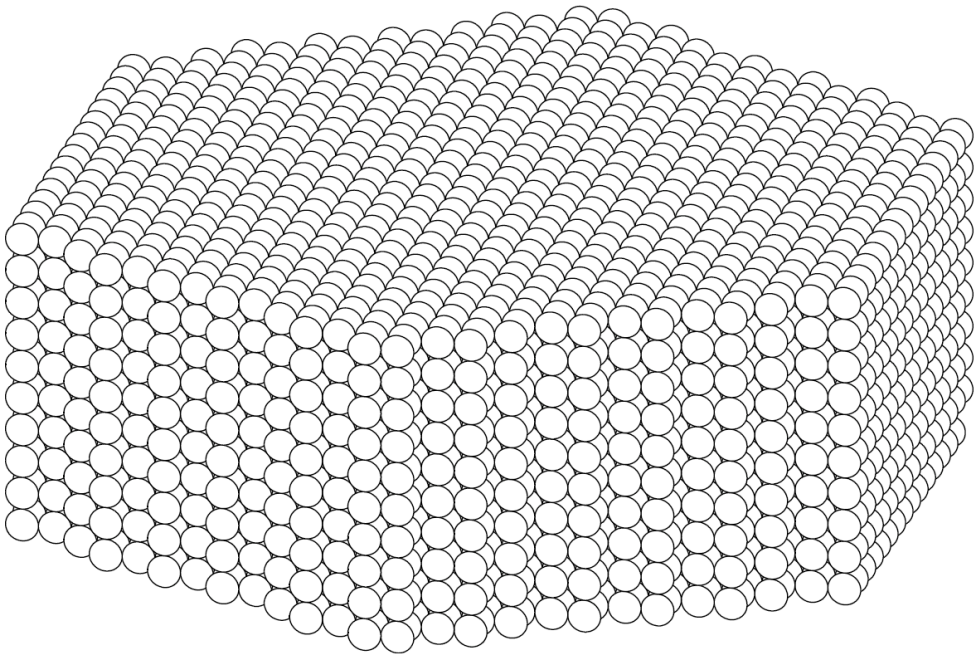

Fig. 9. Representation of a hexagonal plate ice crystal for the DDA computation.

As examples, Figs. 10 and 11 show the scattering phase functions of randomly-oriented large and small ice crystals, computed from the ray-tracing technique and the FDTD method, respectively. For large aggregates shown in Fig. 10., the surfaces of the particles are assumed to be rough. Note that surface roughness for the aggregates results in a smoother phase function in comparison with the pristine crystals such as the columns and plates. The phase function describes the scattered energy of unpolarized incident radiation. It is evident from Fig. 10 that the phase functions of large ice crystals show strong scattering peaks with the exception of the aggregates. The peaks at scattering angle 22° and 46° correspond to the well-known 22° and 46° halos. Such peaks are not observed for small ice crystals.

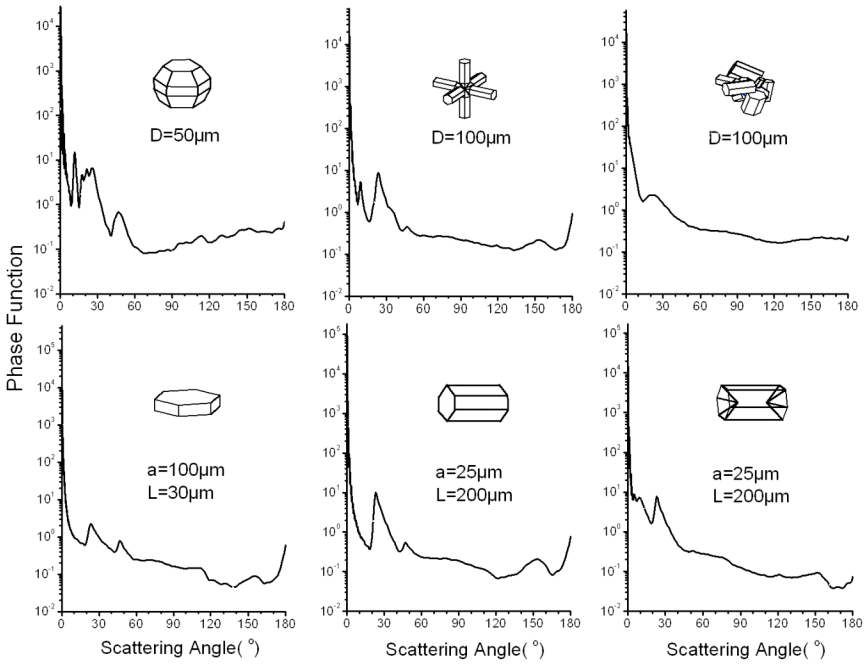

Fig. 10. Comparison of the phase functions computed from the geometric optics method for six ice crystal habits (top row, left to right: droxtals, bullet rosettes, aggregates; bottom row, left to right: plates, solid columns, and hollow columns). Aggregates have surface roughness included in the light scattering computations. Adapted from Yang and Liou (2006).

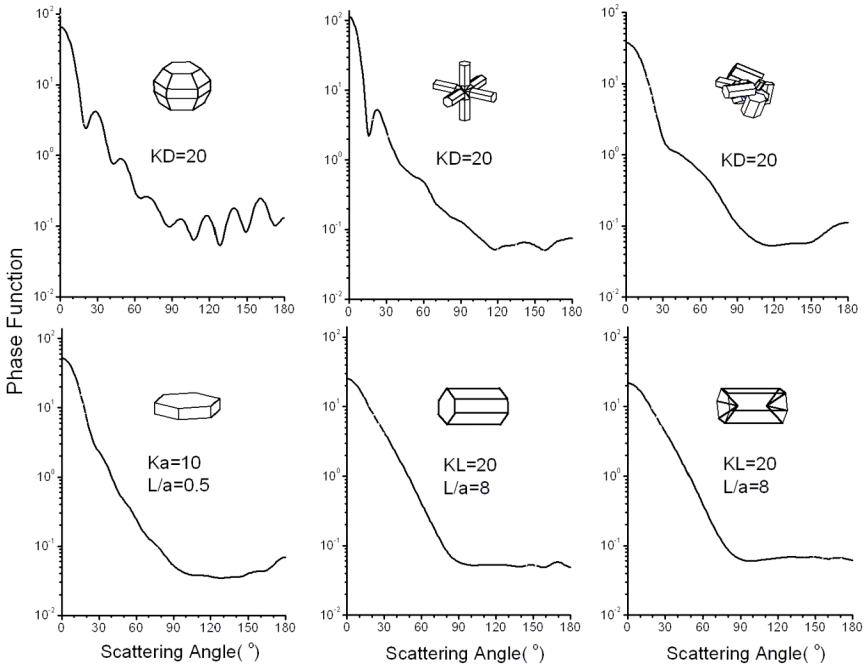

Fig. 11. Comparison of the phase functions computed from the FDTD method for ice ice crystal shapes that are commonly observed in ice clouds. The parameter, D, is the maximum dimension for a droxtal, a bullet rosette, or an aggregate ice crystal. For plates and columns, a denotes the half-width and L is the length (for columns) or thickness (for plates). $K=2\pi/\lambda$ is the wavenumber. Adapted from Yang and Liou (2006).

b. Present state of modeling capability/best approach for light scattering computation

The performances of different numerical methods rely strongly on the shape, size, orientation, and composition (or refractive index) of the particle. The most practical approach at present for computing the optical properties of nonspherical ice crystals may be a combination of FDTD, DDA, T-matrix methods and the ray-tracing technique.

FDTD and DDA are two methods that are applicable to arbitrarily shaped inhomogeneous particles. On a desktop computer, the practical upper limit of size parameter for the application of the FDTD (or DDA) method to the scattering of light by randomly oriented small ice crystals is on the order of 20-30. A comparison study of parallel implementations of DDA and FDTD methods (Yurkin, 2007) shows that DDA is faster when the refractive index m is smaller than about 1.4, while FDTD is more efficient for larger m. According to the spectral variation of the refractive index of ice, DDA may be suitable for the UV and near infrared regions, whereas FDTD for the far infrared region.

Different from FDTD and DDA, which are exact methods for light scattering computation in the framework of the Maxwell theory, the ray-tracing technique is based on the geometric optics, an approximate and asymptotic electromagnetic theory. This method is quite inaccurate if the size parameters are less than 50. Thus, substantial errors may be incurred for moderate sizes where the solutions of the FDTD (or DDA) method and the ray-tracing technique are emerged because the edge effect is not included in the ray-tracing technique. The advantage of this method is that the internal field or near field can be obtained quickly, although not accurate enough. In order to improve the accuracy of optical properties in the region of moderate size parameters, a possible hybrid method with two steps may be used. In the first step, the ray-tracing technique is employed to estimate the internal field within the particle on each grid. This process may not take much CPU time. In the second step, the approximate internal field is going to be substituted into DDA equations as the initial value. As the iteration is executed, the accuracy of the internal field may be improved with the edge effect considered.

2.2 Radiative forcing contrails and contrail-induced cirrus clouds

a. Current state of science

As one of the most visible anthropogenic effects in the atmosphere, contrails and contrail-cirrus are a common sight in the skies over regions with heavy air traffic. Fig. 12 shows the effect of persisting contrails on the diurnal temperature range (Travis et al., 2002). This range tends to be reduced by the occurrence of contrails, which affect the transfer of solar and infrared radiation, as demonstrated by measurements taken around 9/11/01, when all civil and commercial aircraft were temporarily grounded.

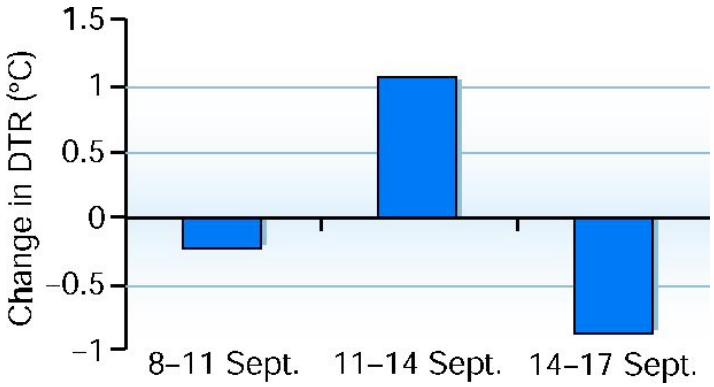

Figure 12. Differences between the average diurnal temperature ranges and the normal values derived from 1971-2000 climatology data for the indicated three-day periods in September 2001 (Travis et al., 2002). All commercial aircraft traffic was grounded in 11-14 September.

Duda et al. (2003) reported that the values of the radiative forcing of global linearly-shaped contrails derived by Minnis et al. (1999) differ from that derived by Ponater et al. (2002) by nearly two orders of magnitude. Figure 13 shows the radiative forcing of contrails calculated by Ponater et al. (2002). In addition, almost all existing studies about contrail radiative forcing focus on linearly-shaped contrails that can be discriminated from natural cirrus in satellite images. These results represent the minimum impact because they do not include the cirrus shields that develop from expanding contrails (Minnis et al. 1998; Duda et al. 2001).

The expansion of contrails into larger-scale cirrus provides another significant effect of contrails on climate, and requires further observational and theoretical modeling studies. We need to investigate the effects of contrail/cirrus coverage and their mean optical thickness to estimate their radiative forcing accurately. The contrail and contrail-induced cirrus radiative forcing depends on the microphysical, macrophysical, and optical properties of contrail and contrail-induced cirrus, as well as the temporal characteristics (i.e., longevity) of these clouds. These uncertainties are discussed in section 3.

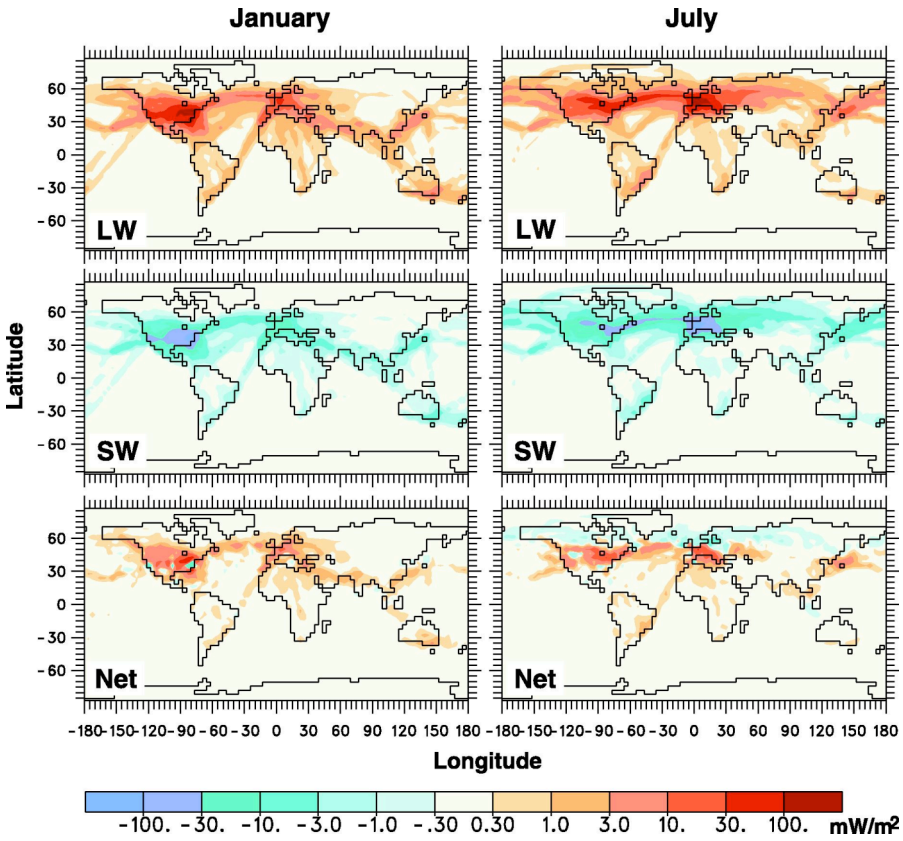

Figure 13. Radiative forcing at the tropopause due to contrails for January and July (Ponater et al., 2002). Top (longwave radiation), middle (shortwave radiation), and bottom (net radiation).

b. Advancements since the IPCC 1999 report

The radiative effects of contrails may be similar to those of natural cirrus clouds because both are ice clouds (Fu and Liou, 1993). Contrails may have significant regional climatic effects (Liou et al., 1990). However, the climate effects which are measured by the radiative forcing of contrails and contrail-induced cirrus are extremely uncertain. In IPCC (1999), a best estimate based on the study of Minnis et al. (1999) of the global distribution of the radiative forcing of contrails observed in 1992 is approximately 0.02 Wm^{-2}. Recently, the global radiative effects of contrails have been further investigated using different datasets, models, and methods (Myhre and Stordal, 2001; Marquart et al., 2003; Fichter et al., 2005; Stuber and Forster, 2007). From these new investigations, the global mean and annual mean radiative forcing due to line-shaped contrails of Minnis et al. (1999) were overestimated. Sausen et al. (2005) reported a value of 0.01 Wm^{-2} as the best estimation of contrail radiative forcing in 2000, which is only half of the value provided in IPCC (1999). Figure 14 shows the annual mean net radiative forcing at the top of the atmosphere for the contrails observed in 1992 with an optical thickness of 0.3 (Minnis et al., 1999). Evidently, the maximum values of contrail radiative forcing are observed over the United States and Europe.

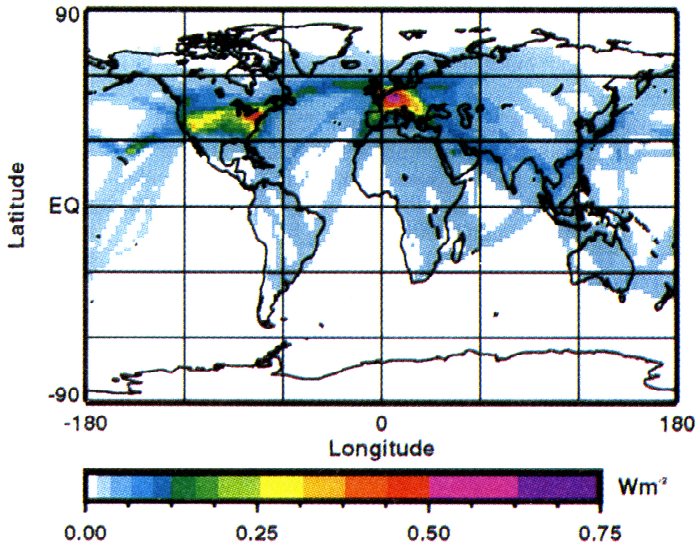

Figure 14. Annual mean net radiative forcing at the top of atmosphere for estimate contrails with an optical thickness of 0.3 in 1999. Adapted from Minnis et al. (1999).

3. Outstanding limitations, gaps and issues that need improvement

3.1 Improvements are needed on the computation of the optical properties of ice crystals

An efficient method at present for computing the light scattering properties of nonspherical ice crystals may be a combination of FDTD, DDA, T-matrix and the ray-tracing technique. The computational efficiency of existing computer codes (FDTD and DDA, in particular) needs to be substantially improved for practical applications.

3.2 Uncertainties in Estimates of Radiative Forcing of Contrails and Contrail-induced Cirrus Clouds

3.2.1 Contrail and Contrail-induced Cirrus Covers

The estimates of contrail and contrail-induced cloud covers are important since air traffic increases 2-5% annually (Minnis et al., 1999). However, global contrail and contrail-induced radiative forcing is difficult to estimate since the global mean contrail and contrail-induced coverage is poorly known. Sausen et al. (1998) estimated the global mean cover by linearly-shaped contrails to be about 0.1%. The value of 0.02 Wm^{-2} for the global and annual mean radiative forcing by line-shaped contrails (Minnis et al., 1999) was based on this value of contrail cover. Ponater et al. (2002) reported that the annual average for visible contrail coverage amounts to 0.07%. In regions with high air traffic density, time mean coverage of more than 2% has been found (Ponater et al., 2002).

The uncertainty in contrail coverage estimates has been illustrated by the results from different detection methods (Duda et al., 2003). There are two methods generally used to infer contrail coverage: One approach uses a parameterization in a numerical weather

prediction model to diagnose contrails based on the ambient conditions (Sausen et al., 1998; Ponater et al., 2002; Duda et al., 2003). The other approach is based on satellite imagery analysis (Bakan et al., 1994; Mannstein et al., 1999; Palikonda et al., 1999; Meyer et al., 2002). The contrail coverage from these approaches provides different estimates of contrail coverage and spatial distribution. But in general, both approaches depend on the air traffic density. Boucher (1999) and Fahey et al. (1999) showed that cirrus occurrence and coverage tend to increase in regions of high air traffic compared with the rest of the globe (IPCC). Figure 15 shows the trends in cirrus coverage from 1971 to 1995 and estimated 1992 linear contrail coverage (Minnis et al., 2004). It is clear that the largest concentrated increases occurred over the northern Pacific and Atlantic and roughly corresponded to the high air traffic densities. Moreover, the regional and local climate response to the regional and local air traffics with high aviation emissions is different from the global mean radiative forcing that is highly important to the global mean climate change.

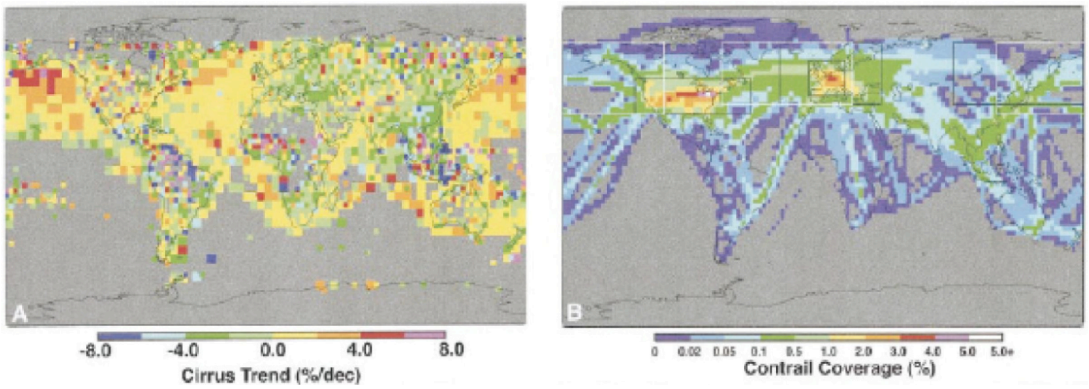

Figure 15. (a) Trends in cirrus coverage from 1971 to 1995 and (b) estimated 1992 linear contrail coverage. Adapted from Minnis et al. (2004).

Stordal et al. (2005) estimated the trends in cirrus cloud cover on the basis of 16 years of data from the International Satellite Cloud Climatology Project (ISCCP, Rossow and Schiffer, 1999). The trends were then spatially correlated with aircraft density to determine the variations in cirrus cloud cover due to aircraft traffic. Cirrus cloud amount increases were reported to accompany an increase in aircraft in the period of 1984-1999. They found that the strongest influence on cirrus clouds occurs in the regions with highest aircraft traffic. However, they also documented that the relationship between cirrus cloud cover and aircraft density was uncertain and they could not draw firm conclusions or quantify the effect with high certainty. Figure 16 shows the correlation coefficients between trends in cirrus cloud amount from ISCCP and aircraft traffic density (Stordal et al., 2005). The correlations are moderate and many other factors may also have contributed to variations in cirrus cloud amount. Their conclusions were based on monthly mean data, and they suggested the use of daily data to improve their results.

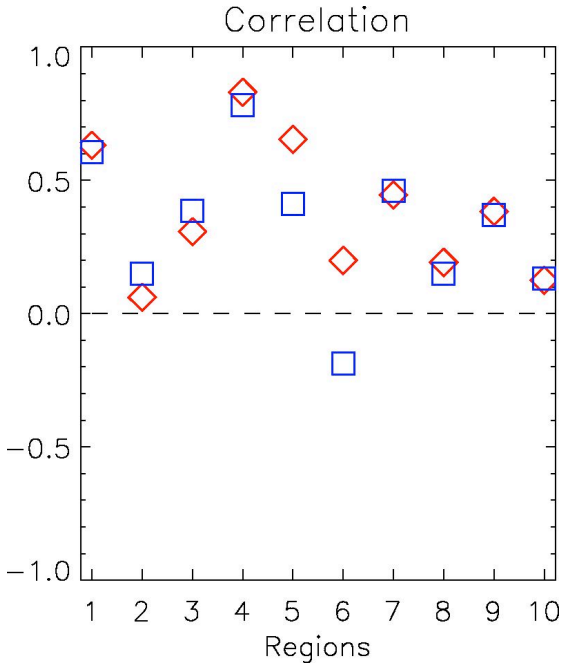

Figure 16. The correlation coefficients between trends in cirrus cloud amount from ISCCP and aircraft traffic density over chosen ten regions. Diamond and square indicate two different methods to determine the cirrus clouds. Adapted from Stordal et al. (2005).

3.2.2. Contrail and Contrail-induced Cirrus Optical Thicknesses

The optical thickness determines in large part of the radiative forcing of contrails and contrail-induced cirrus. The optical thickness of contrails is typically between 0.1 and 0.5 (e.g., Sassen, 1997; Minnis et al., 1998), and can sometimes be as low as 3.0×10^{-5} (Schröder et al., 2000). Larger values of optical thickness may approach or exceed 1 at warmer temperatures (up to -30ºC) (Schumann and Wendling, 1990; Gayet et al., 1996). Different mean contrail optical thicknesses have been used to study the radiative forcing of contrails globally and regionally. For example, an optical thickness of about 0.1 was assumed by Stuber and Forster (2007) for a global mean; 0.15 was used by Ponater et al. (2002) for a global mean; 0.2 was a value given over the life cycles of contrails that developed into cirrus clouds (Duda et al., 2004). Minnis et al. (2002) estimated an optical depth of 0.26 for a large area of contrails from initiation to dissipation; Palikonda et al. (2004) found a similar value of 0.26 using an automated analysis data from two satellites during all of 2001; 0.3 was used by Myhre and Stordal (2001) for a global mean; and 0.52 was used by Meerkötter et al. (1999), which combined with a global mean contrail cover of 0.1%, leads to 0.01 to 0.03 Wm^{-2} daily and annual mean radiative forcings.

The dependence of radiative forcing on the assumed contrail optical thickness is shown in Figure 17 (Meerkötter et al., 1999). At the top of atmosphere, the longwave forcing is larger than the shortwave forcing. Thus, the radiative forcing of contrail and contrail-induce cirrus is positive and generally increases with increasing optical thicknesses. However, at the surface, the longwave forcing is smaller than the shortwave forcing, which results in negative radiative forcing.

As optical thickness increases for naturally-occurring cirrus, the net radiative forcing at the top of atmosphere decreases. Hong et al. (2007b) analyzed three years of MODIS data, it was found that the mean optical thickness and effective particle size of tropical ice clouds are about 8 and 50 μm, respectively. The radiative forcing at the top of the atmosphere and surface by ice clouds is shown in Figure 18 as a function of optical depth. The figure shows the impact of optical thicknesses on the radiative forcing.

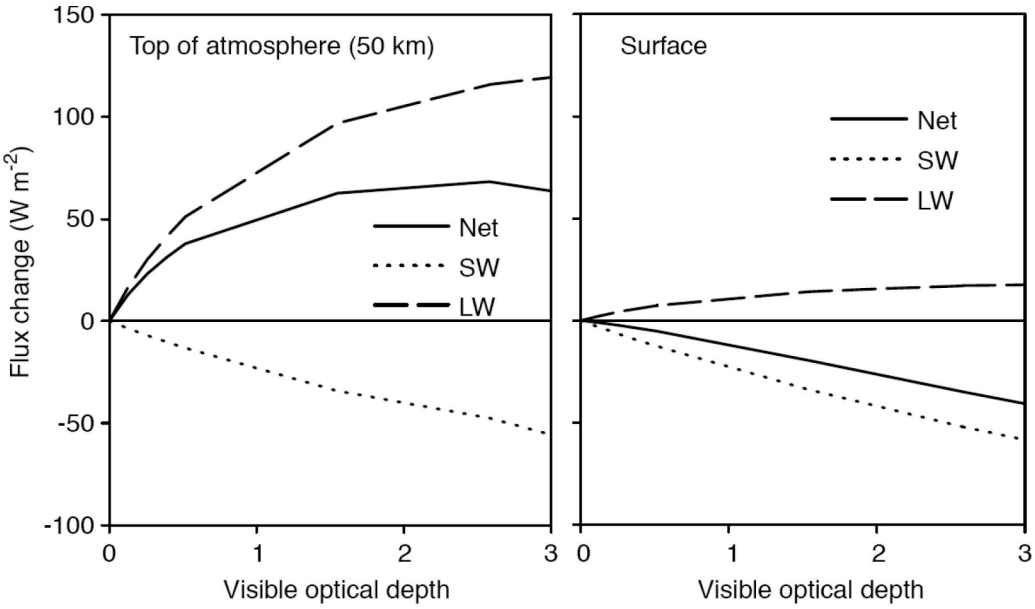

Figure 17. Computed shortwave and longwave net fluxes for 100% contrail cover at the top of atmosphere and at the surface as a function of optical thickness of contrails Adapted from Meerkötter et al. (1999).

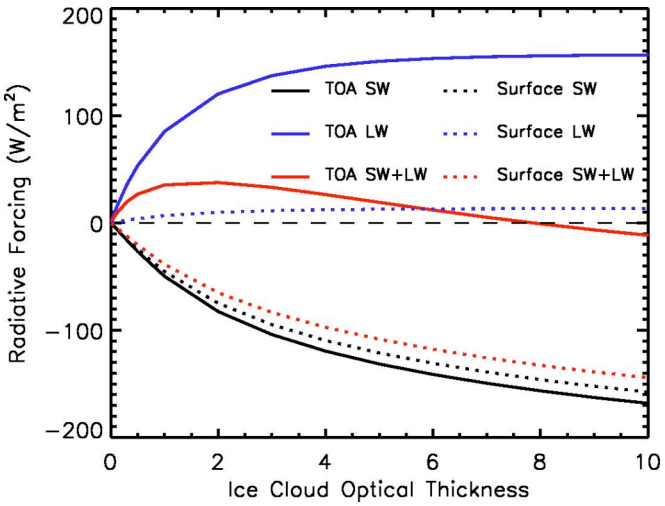

Figure 18. Computed shortwave and longwave net fluxes for 100% cirrus cover at the top of atmosphere and at the surface as a function of optical thickness of cirrus (Hong et al., unpublished).

The contrail optical thickness also varies geographically, which affects the distribution of the radiative forcing. Figure 19 shows the spatial and interannual variability of the optical thickness at pressures of 200 and 250 hPa (Ponater et al., 2002). The optical thickness of contrails in the extratropical regions is considerably smaller in winter (mostly less than 0.1) than in summer.

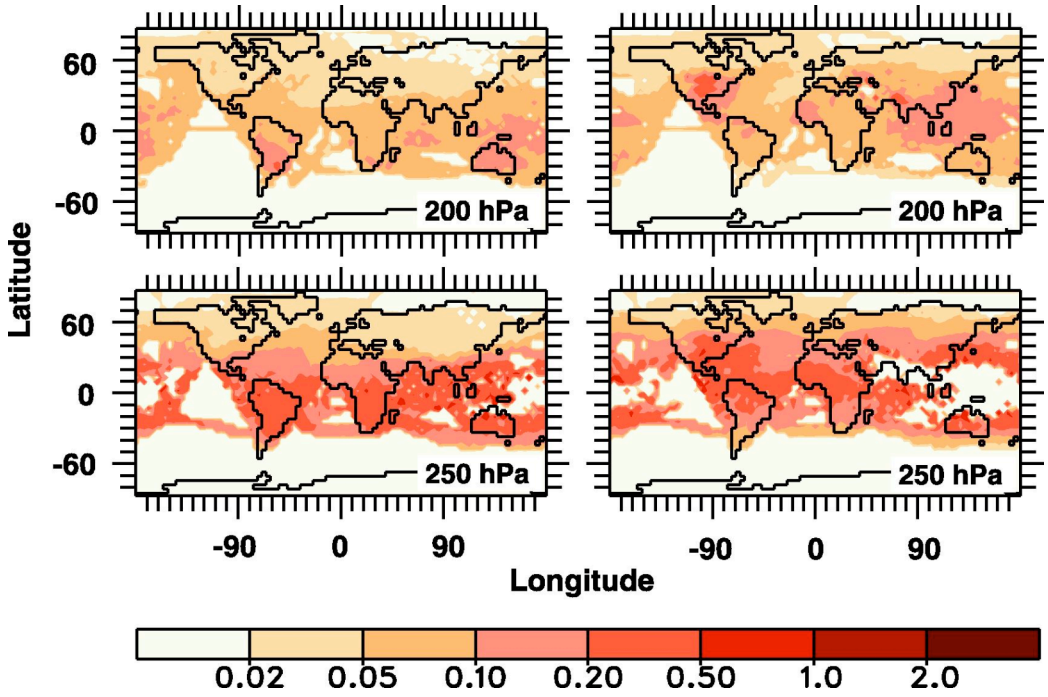

Figure 19. The geographical and seasonal distributions of optical thickness for visible contrails at 200 and 250 hPa. Left is for January and right for July. Adapted from Ponater et al. (2002)

3.2.3. Ice Particle Sizes in Contrail and Contrail-induced Cirrus

Significant problems exist with the measurement of small ice particles as reported by Heymsfield et al. (2006) and Garrett (2007). The ice particle sizes in contrail and contrail-induced cirrus clouds can range from a few microns to hundreds of microns or more. Measuring the ice particle sizes over this range requires several instruments (e.g., Schröder et al., 2000), such as the forward scattering spectrometer probe (FSSP), the optical array probe (OAP), high-volume precipitation spectrometer (HVPS), cloud virtual impactor (CVI), Hallett-type repicator (REP), cloud intergrating nephelometer (CIN), and most recently the small ice detector (SID).

The agreement between measurements from the different instruments has not always been good. Specially, the measurement of small ice particles strongly depends on the instrument (e.g., Heymsfield et al., 2006; Garrett, 2007). Heymsfield et al. (2006) compared the in situ direct and indirect measurements of extinction coefficient, as well as

measured values from lidar. They reported that the direct-extinction measurements used by Garrett et al. (2003) are overestimated by a factor of 2 to 2.5.

Figure 20 shows the extinction coefficient estimated from the FSSP and from the particle probes, as well as values measured directly by the CIN probe. Heymsfied et al. (2006) speculated that the source of the errors is from large ice particles that shatter on the housing of the instrument aperture, and subsequently intersect the sample volume. Shattering does not affect ice mass density but increases total surface area, thereby affecting the inference of extinction coefficient. Heymsfield et al. (2006) concluded that indirect measurements of ice particle sizes are the most accurate.

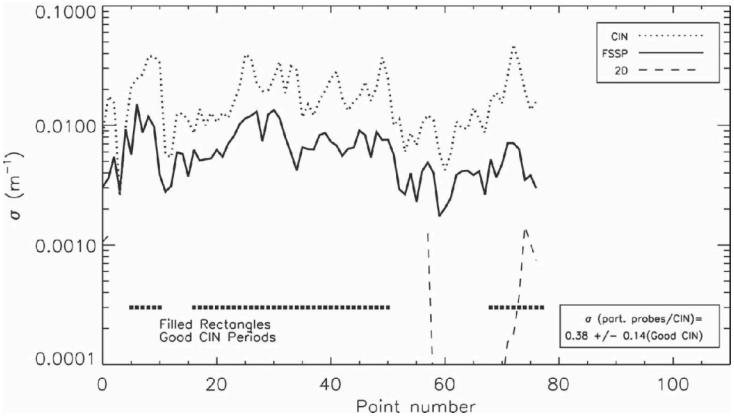

Figure 20. Comparison of extinction derived from FSSP to measurements from the CIN probe. Adapted from Heymsfield et al. (2006).

Garrett (2007) reassessed the analysis and conclusions of Heymsfied et al. (2006). It was there found that the discrepancy between the CIN and particle probe measurements of extinction coefficient during CRYSTAL-FACE was not from shattering. The measurements of ice particle sizes and optical thickness of cirrus clouds derived using a CIN probe were in agreement with those derived from a variety of passive remote sensors employing different retrieval algorithms. It is further confirmed that measurements from different FSSP-type probes can differ greatly in their estimation of ice water content and extinction coefficient although they operate on the same basic principles. Noel et al. (2007) compared extinction coefficients retrieved in ice clouds from lidar observations using a CALIPSO-like algorithm to in-situ measurements from the CIN during CRYSTAL-FACE. The results show a very good agreement between both instruments, as evident from Figure 21. Despite these achievements, the microphysical and optical properties of small ice particles need to be further investigated.

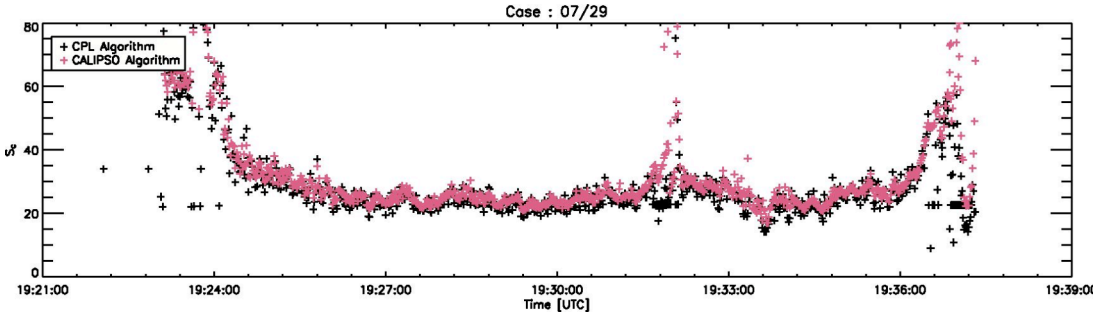

Figure 21. Lidar ratio from the cloud physical lidar (black) CALIPSO algorithm (pink) Adapted from Noel et al. (2007).

3.2.4. Diurnal Variations of Air Traffic

Solar radiative forcing varies substantially with solar zenith angley (Myhre and Stordal, 2001). Figure 22 from Myhre and Stordal (2001) shows how the solar radiative forcing varies with solar zenith angle for different values of surface albedo with a fixed mid-latitude summer atmosphere. The strongest negative forcing was found at high solar zenith angles between 75°-80° (Meerkötter et al., 1999; Myhre and Stordal, 2001). The strong forward scattering of larger ice particles leads to a decrease in backscattering at low solar zenith angles (Haywood and Shine, 1997; Myhre and Stordal, 2001). Myhre and Stordal (2001) also investigated the diurnal variation in the global shortwave radiative forcing performed for 1% homogeneous global contrail cover, with results shown in Figure 23. The forcing during sunrise and sunset substantially differs from that at noon.

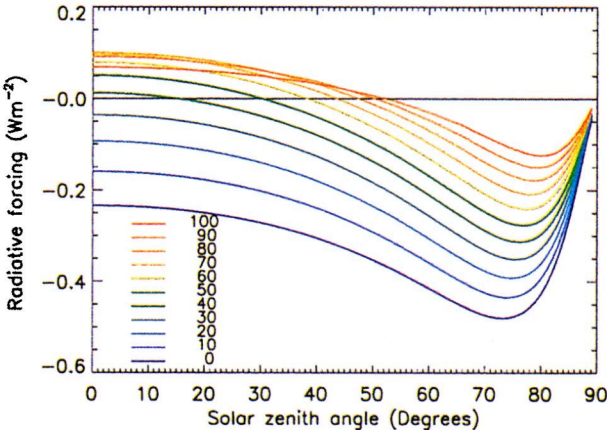

Figure 22. Solar radiative forcing of contrails as a function of solar zenith angle for various values of surface albedo (0-100%) (Myhre and Stordal, 2001).

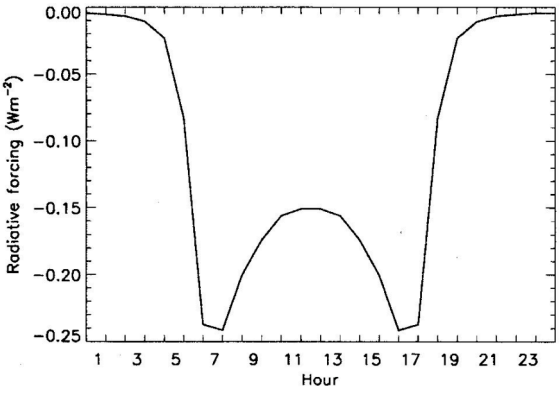

Figure 23. Annual globally mean shortwave radiative forcing due to contrails as a function of local time for a globally homogeneous cloud cover of 1%. Adapted from Myhre and Stordal (2001).

The diurnal variations of contrail coverage and properties are also important for the mean radiative forcing because solar radiative forcing is restricted to the daytime period. The diurnal coverage ratio may be expressed as a ratio of total daily contrail coverage to daytime-only coverage. Diurnal coverage ratios of contrails were found to be about 2 over Europe (Bakan et al., 1994) and 3 over central Europe (Mannstein et al., 1998). The diurnal contrail coverage ratio was consistent with a global mean noon-midnight traffic ratio of 2.8 (Schmitt and Brunner, 1997).

However, the diurnal variation of air traffic is often neglected for contrail radiative forcing (e.g., Marquart et al., 2003; Fichter et al., 2005). The effect of diurnal variations of air traffic on contrail radiative forcing over southeast England was investigated by Stuber et al. (2006). The flights during the nighttime were found to have a disproportionate effect on the annual, diurnal mean contrail radiative forcing because the longwave warming is not offset by any shortwave cooling.

To determine the effects of diurnal variations of air traffic on global mean contrail radiative forcing, Stuber and Forster (2007) calculated a diurnally resolved 3-D distribution of contrail cover. The radiative forcing was calculated for this contrail cover distribution with an assumed constant contrail optical thickness. It was found that less than 40% of the global distance traveled by aircraft is due to flights during local night time and that neglecting diurnal variations in air traiffic/contrail coverage by assuming a diurnal mean contrail coverage can overestimate the global mean radiative forcing by up to 30% (Stuber and Forster, 2007). Figure 24, from Stuber and Forster (2007), shows (a) percentage of flights during local night time and (b) a geographic distribution of the annual mean relative underestimation or overestimation of contrail radiative forcing due to neglect of the diurnal variations of air traffic.

(a)

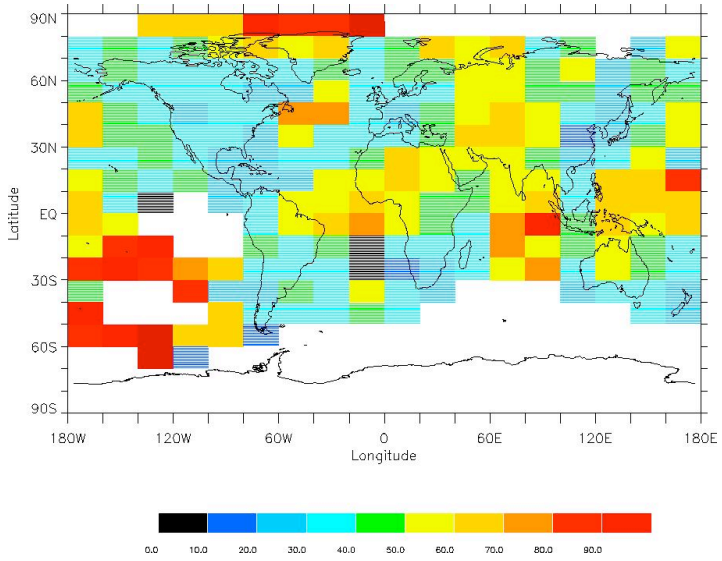

(b)

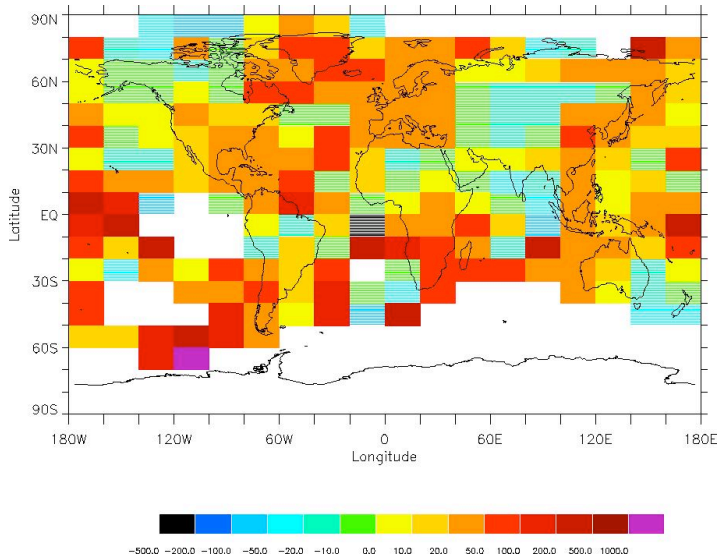

Figure 24. (a) Percentage of flights during local night time. (b) Geographical distribution of the percentage overestimation/underestimation of annual mean contrail radiative forcing resulting from neglecting the diurnal cycle of air traffic. Adapted from Stuber and Forster (2007).

For those locations with significant local forcing, the net radiative forcing was overestimated when the diurnal variation of air traffic was neglected. The increase of the net forcing for these regions was due to the increasing number of flights during local nighttime in comparison with a diurnally uniform distribution of flights.

3.2.5. Detection of Contrail and Contrail-induced Cirrus

Split-window brightness temperature difference techniques (Prabhakara et al., 1988; Parol et al., 1991; Gothe and Grassl, 1993; Duda and Spinhirne, 1996; Duda et al., 1998)

have been used to estimate optical and microphysical properties of thin cirrus and contrails. Much work has been done to understand the retrieval accuracies of these techniques (Gao et al., 1993; Stubenrauch et al., 1999; Rädel et al., 2003; Hong et al., 2007a). For example, Hong et al. (2007a) investigated the effect of the ice cloud geometrical thickness on the retrieval of optical thickness and effective particle size using split-window bands at 8.5 and 11 μm (or 12 μm). The optical thickness in the IR depends strongly on cloud geometrical thickness, and slightly on cloud effective particle size.

Gao et al. (1998) revealed that the narrow channels near the centers of the 1.38 and 1.88 μm water vapor absorption bands are useful for detecting thin cirrus clouds owing to the strong water vapor absorption in the lower atmosphere. The two channels have been used to detect the optical thickness and effective particle size of contrail cirrus by Gao, Meyer, and Yang (2004). Figure 25 shows the observations of 1.38 and 1.88 μm for a contrail cirrus and the retrieved optical thickness and effective particle size. This method is effective for detecting contrail and contrail-cirrus, thereby, investigating the regional or global mean distribution of contrails and cirrus covers and their optical depths, and measuring the variations of properties over different time scales (diurnal, monthly and annual). However, the 1.88 μm is not measured by any existing satellite sensor, although the MODIS band 26 is centered within the 1.38-μm water vapor band.

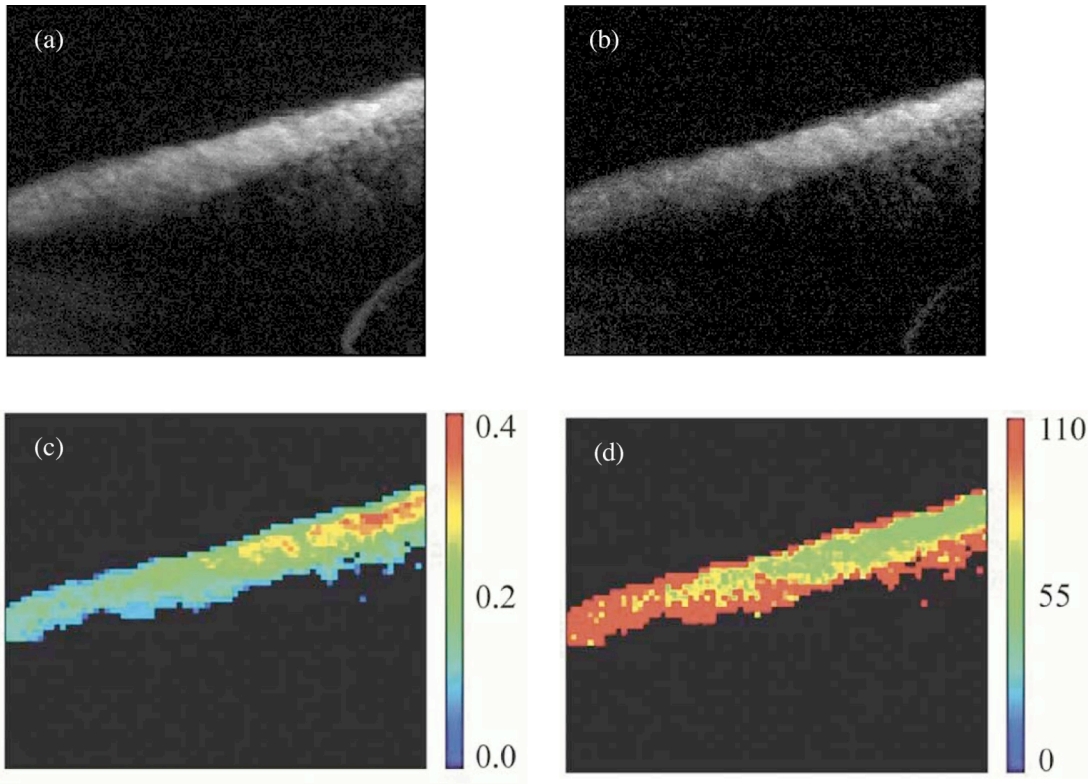

Figure 25. (a) and (b) are for 1.38 and 1.88 μm images for a contrail cirrus, respectively, (c) and (d) are for retrieved optical thickness and effective particle size (in units of μm), respectively (Gao et al., 1998).

3.2.6 Dependency of Different Types of Aerosols

The ability of aerosols to promote ice formation and the aerosol number density are key factors controlling ice clouds and their radiative forcing. Mangold et al. (2005) investigated the ice water content, ice crystal number concentration, and particle sizes during ice cloud formation experiments for different temperatures and types of aerosol particles. It was found that ice water content generally decreased with decreasing temperature. Figure 26 shows the maximum ice water content for different aerosols as ice nuclei for temperatures ranging from 200 K to 225 K (Mangold et al., 2005). No clear influence of the aerosol type on the ice water content was found generally. The ice crystal number increased and their sizes decreased with decreasing temperature for all aerosol types.

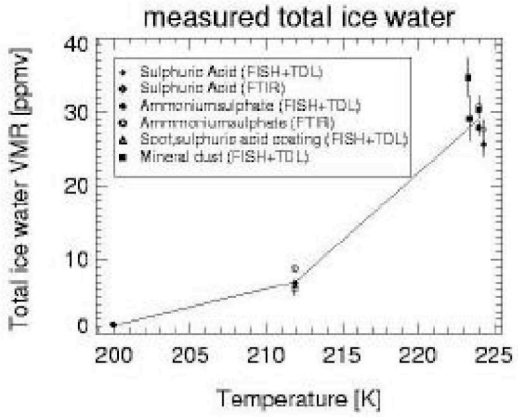

Figure 26. The maximum ice water content for different aerosols as ice nuclei for temperatures ranging from 200 K to 225 K (Mangold et al., 2005).

Contrail particles have been found to contain soot (Kuhn et al., 1998; Petzold et al., 1998; Störm and Ohlsson, 1998a, 1998b). The effect of aircraft soot on ice cloud formation in the absence of contrails is highly complex and depends on a wide variety of aerosol emission and environmental parameters (e.g., Petzold et al., 1997; Kuhn et al., 1998; Störm and Ohlsson, 1998a, 1998b; Kärcher et al., 2007). The difficulty in assessing the role of aircraft soot in ice cloud formation is in separating its influence from those of other aerosols and unambiguously demonstrating that ice nucleates on the exhaust soot particles or those affected by the soot, sulfur, and organic emissions by coagulation and condensation (Kärcher et al., 2007). Kärcher et al. (2007) investigated the role of soot aerosols in ice cloud formation with a combination of process-oriented modeling and evaluation of laboratory results of heterogeneous ice nucleation. They suggested two principal scenarios: "high concentrations of original soot emissions could slightly increase the number of ice crystals; low concentrations of particles originating from coagulation of emitted soot with background aerosols could lead to a significant reduction in ice crystal number." However, a fundamental understanding of the ice nucleation efficiency of soot particles is still lacking. Uncertainties remain in modeling

the interaction between direct (contrail cirrus) and indirect (soot-induced cirrus) effects on ice clouds (Kärcher et al., 2007).

Soot within or on an ice particle affects the refractive index of the particle, and hence influences the scattering properties. In turn, this may result in differences in radiative forcing. Chylek and Hallett (1992) documented that the importance of the soot is associated with the type of mixing (external or internal) and the volume fraction of soot enclosures. The question remains whether the black carbon particles are incorporated into contrail ice crystals or deposited on the ice crystal surface, and this is critical for understanding the contrail formation process (Kuhn et al., 1998). Kuhn et al. (1998) found that contrails contain a mixture of pure ice particles, black carbon aerosol, and an internal mixture of these components, using the measurements from the SULFUR-4 experiment in March 1996 over southern Germany.

Figure 27 shows the major components of a young contrail (Kuhn et al., 1998). The contrail was found to be a mixture of 15% ice particles, 32% ice with black carbon, 24% black carbon, and 29% unknown aerosols. The ice with black carbon was found to contain a black carbon volume fraction of 15-20%. Knowledge of the composition is critical for obtaining accurate refractive indices of ice particles and aerosols in the contrails. It is also important to know the background atmospheric composition, such as humidity.

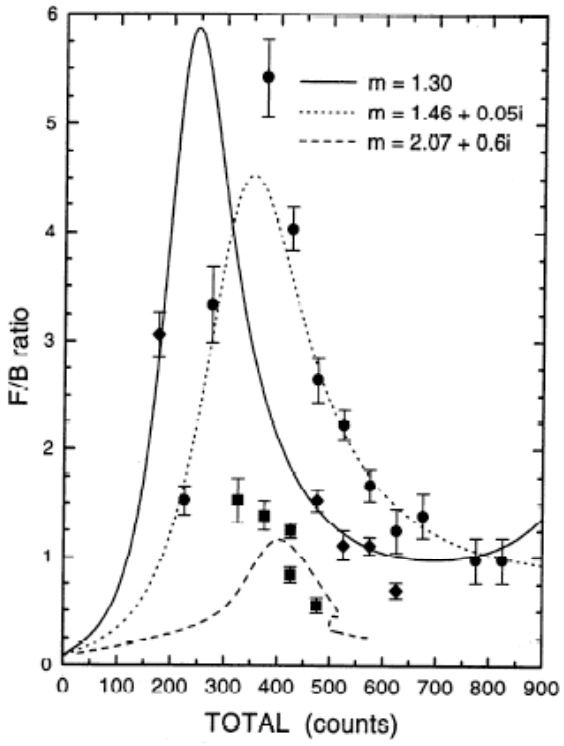

Figure 27. Major components of a young contrail. F/B ratio is the ratio of forward to backward scattered radiation. Ice has a refractive index of 1.30, black carbon has a refractive index of 2.07+0.6i, and ice with black carbon has a refractive index of 1.46+0.0i. Adapted from Kuhn et al., (1998).

3.2.7 Contrails Occurring in Cirrus Clouds

Since aircrafts generally fly at the same heights at which ice clouds naturally occur, contrails often co-exist with cirrus clouds. Immler et al. (2007) found contrails are often embedded in a partly subvisible cirrostratus. One might expect a difference in microphysical and optical properties for contrails embedded within a cirrus deck from that of contrail-induced cirrus, but no related studies can be found that explore this issue.

The effect of dynamical variability in cirrus cloud formation was investigated by Kärcher and Störm (2003). They found that vertical velocities and mesoscale variability in vertical velocities could significantly modify the probability distribution of cirrus ice crystal concentrations. Figure 28 shows the obvious effect of variability in updraft velocity on ice particle number densities.

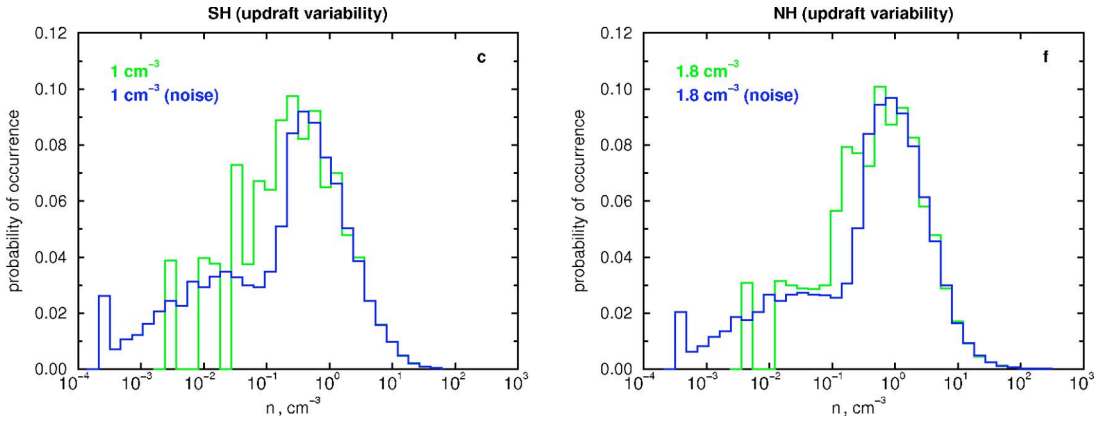

Figure 28. The effect of updraft variability ice particle concentrations in the southern hemisphere (SH) and northern hemisphere (NH) from Kärcher and Störm (2003).

Figure 29 shows a schematic of the dynamic, chemical, and microphysical processes involved in the formation of an internal mixture of soot particles containing black carbon from an aircraft exhaust plume (Kärcher et al., 2007). This scheme was applied to a Lagrangian plume model with interactive entrainment of constituents present in ambient air, gas phase sulfur chemistry and condensation, and coagulation between particles of different size and composition to understand the factors controlling the generation of internally mixed aircraft-soot particles. This scheme was designed for contrails occurring in an otherwise clear sky, not for contrails occurring in already-existing cirrus clouds. It is still unknown what changes would need to be adopted for the scheme for contrails occurring in already existing cirrus clouds. This requires more direct in situ observations, laboratory measurements, and theoretically studies.

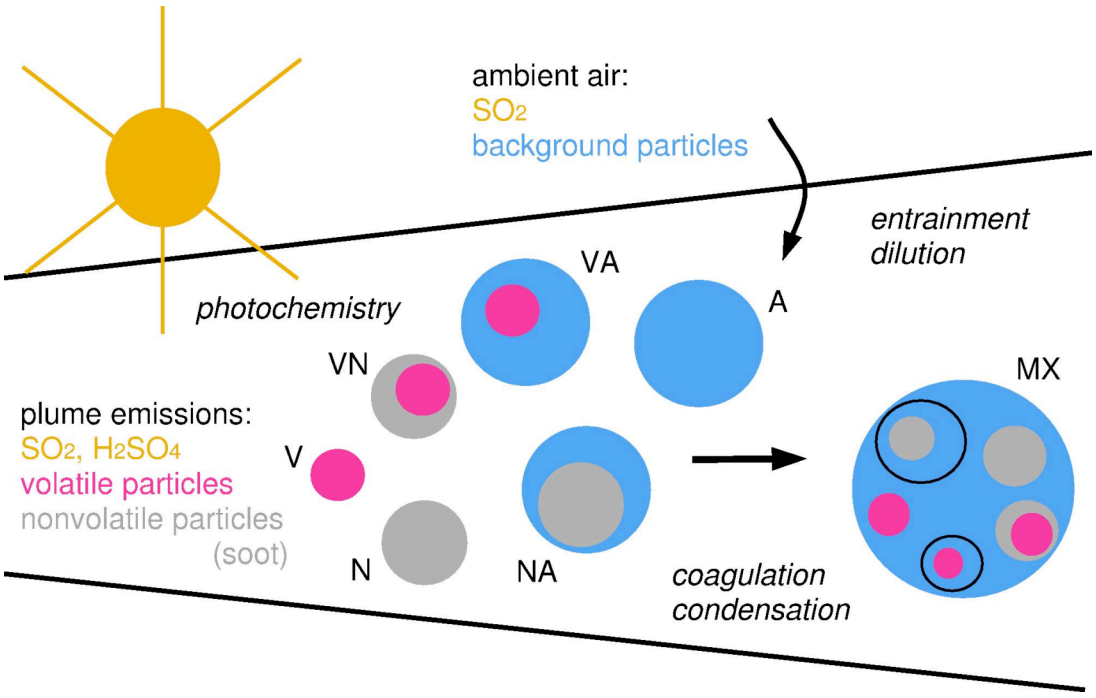

Figure 29. Schematic of the dynamical, chemical, and microphysical processes involved in the formation of internally mixed soot particles containing black carbon from various sources in dispersing aircraft exhaust plumes. V, aircraft-emitted volatile aerosols; N, nonvolatile aerosols; A, entrained background aerosols; VN, coagulated particle resulting from V+N; VA, coagulated particle resulting from V+A; NA, coagulated particle resulting from N+A; MX, coagulated particle resulting from all above particles. Adapted from Kärcher et al. (2007).

3.2.8. Cloud Tops and Physical Thicknesses of Contrail and Contrail-induced Cirrus Clouds

Properties including cloud top height, the cloud vertical distribution, and the properties of each cloud layer within the distribution can also affect cirrus radiative forcing. As pointed out by Sassen and Campbell (2001), "What is currently known of the climatic impact of cirrus has come from theoretical simulations based on idealized cloud macrophysical and microphysical inputs, and a number of radiative transfer approximations."

Different techniques have been used to measure cloud heights, including passive radiometric measurements in the visible, near-infrared, and infrared spectrum (i.e., satellite imagers, sounders, and interferometers) as well as active measurements from lidars. Differences in cloud-top pressure/height results from lidar and the CO_2-slicing method (used for MODIS and HIRS data products) have been shown by Frey et al. (1999) for both single-layered and multilayered clouds. Figure 30 shows the histogram of differences between lidar and CO_2-slicing cloud heights.

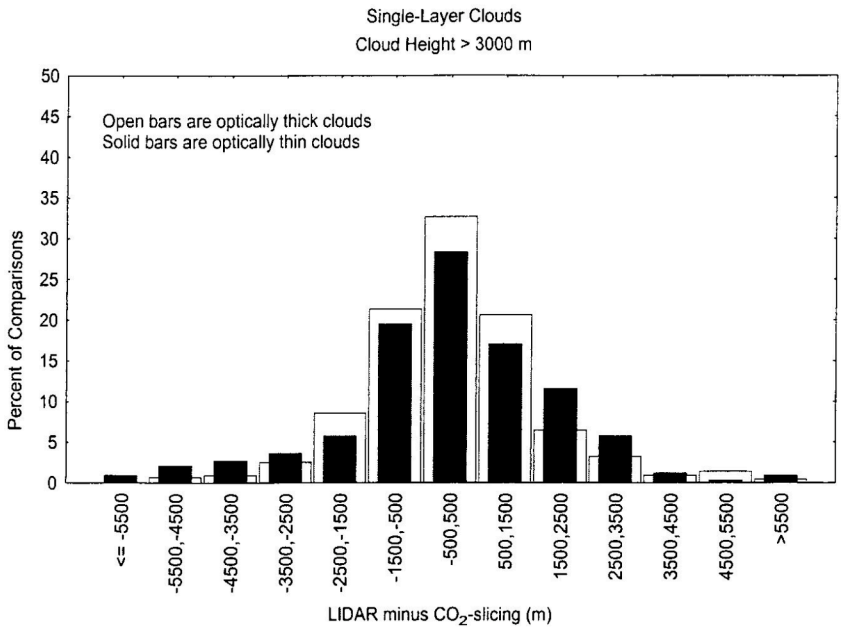

Figure 30. Histogram of differences between lidar and CO2-slicing cloud heights in meters. Clouds are single-layer with tops > 3000 m. Open bars represent optically thick clouds, while solid bars show optically thin cloud retrievals (Frey et al., 1999).

It was found that the tops of contrails and contrail-induced cirrus clouds are generally at 9-12 km (e.g., Sassen and Hsueh, 1998; Meerkötter et al., 1999; Atlas et al., 2006). The geometrical contrail thickness of contrails was found to be in the range of 50-500 m using high-resolution depolarization lidar studies during SUbsonic aircraft: Contrail and Cloud Effects Special Study (Sassen and Hsueh, 1998). Figure 31 shows a series of spreading contrails between 7.5-11.0 km (Atlas et al., 2006). Different cloud top temperatures and physical thickness result in differences in longwave radiative emission and reflectance of solar radiation (Hong et al., 2007b), and therefore affect the total radiative forcing.

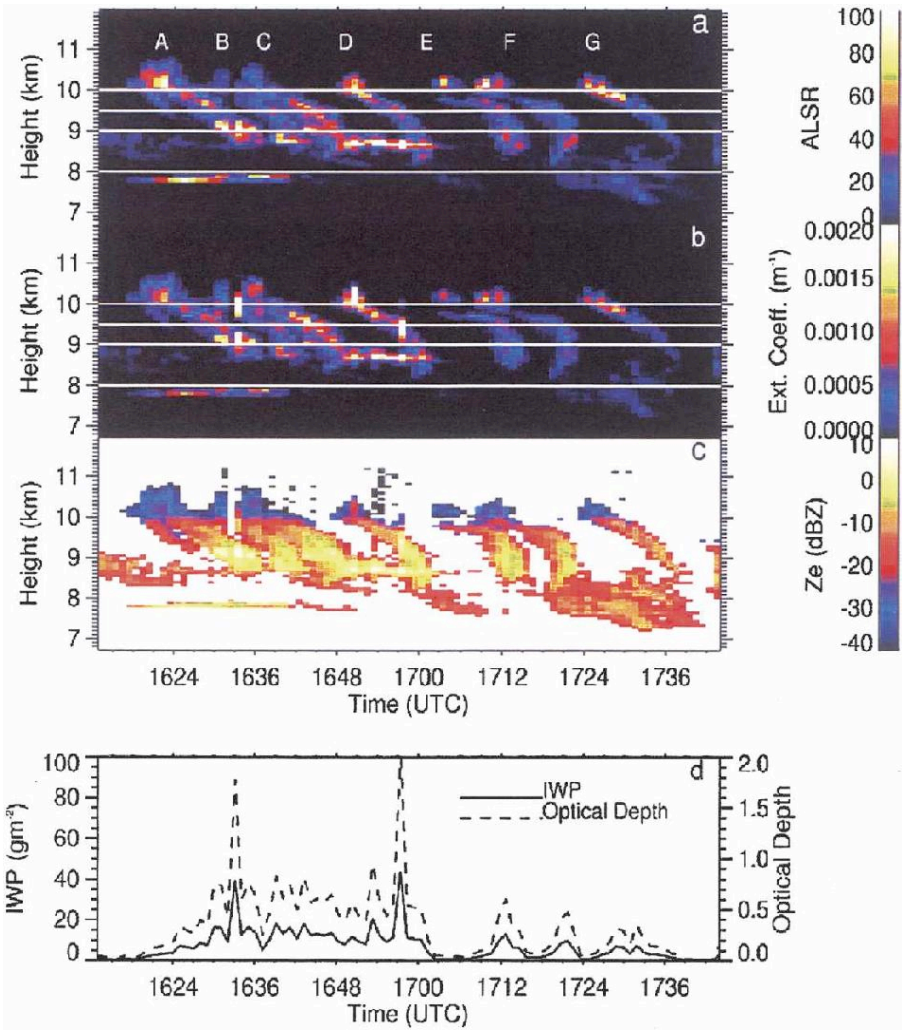

Figure 31. Lidar observations of contrails for (a) attenuated lidar scattering ratio, (b) extinction coefficient, (c) estimated radar reflectivity factor, and (d) corresponding optical thickness. Adapted from Atlas et al. (2006).

Kärcher and Störm (2003) investigated the effects of updraft velocity variability on the formation of ice clouds based on the probability of occurrence of ice crystal number densities. However, their study did not consider the influence of updraft variability on the macrophysical properties of contrails. The processes driving contrail spreading are horizontal diffusion and vertical shear of the horizontal wind (Jensen et al., 1998). Their simulations show that not only the crystal growth, microphysical and optical properties of contrails are strongly dependent on wind shear, but also the vertical distribution and horizontal spreading. However, those studies are hindered by a shortage of in situ observations. The Cloud–Aerosol Lidar Infrared Pathfinder Satellite Observation (CALIPSO) satellite as a part of A-Train (Winker et al. 2003) can provide global observations of contrails and contrail-induced cirrus clouds. Analysis of the CALIPSO products is relatively recent, and depends on the rapid maturation of officially released cloud products.

3.2.9. Representation Contrails and Contrail-induced Cirrus Clouds in GCMs

There are only a few studies that have attempted to determine the climate impact of contrails from general circulation model (GCM) simulations (Ponater et al., 1996; Rind et al., 1996, 2000). Those studies estimated the climate impact of a cirrus cloud perturbation introduced by more or less artificial means. Ponater et al. (2002) developed an online parameterization for contrails that was based on a thermodynamic approach (Schmidt-Appleman theory) adapted to the cloud parameterization scheme of the ECHAM4. However, the radiative forcing of the contrails from the ECHAM4 with the contrail parameterization is substantially smaller than the best estimate given by Minnis et al. (1999) and IPCC (1999). Ponater et al. (2002) documented the potential uncertainties of the model results, which include the dependency of ice water content, ice particle size, and the radiative effect of the simulated contrails on ambient parameters such as temperature, humidity, cirrus frequency, surface albedo, and solar zenith angle. They also suggested a classification approach based on the simulated range of contrail properties for various ambient conditions to reduce the uncertainties of their model results.

The contrail parameterization scheme of Poneter et al. (2002) has also been implemented in the IFSHAM model developed at the Danish Meteorological Institute (Guldberg, 2003). The results from the IFSHAM model and Poneter et al. (2002) were compared to radiative forcing estimates of Guldberg (2003). The global mean of the net radiative forcing was found to be almost a factor of ten less in the IFSHAM model with respect to those from the ECHAM4. Also, there are large areas over Europe and USA with negative net radiative forcing where the net radiative forcing is positive in the ECHAM4 (Ponater et al., 2002; Marquart et al., 2003). Figure 32 shows the annual net radiative forcing at the top of atmosphere from the IFSHAM (Guldberg, 2003) and the ECHAM4 (Marquart et al., 2003). Marquart and Mayer et al. (2002) explained the differences as being caused by a problem of the longwave radiation scheme in ECHAM4 which is different from that used in the IFSHAM model. But Guldburg (2003) suggested further investigation, finding that the contrail effective radii and ice water path from the IFSHAM model are smaller than those in Ponater et al. (2002). The influence of those parameters on the contrail radiative forcing is needed to determine by more model experiences.

The GCM parameterization scheme of contrails by Ponater et al. (2002) did not include a contrail-cirrus feedback due to the additional ice water formation caused by the infusion of aerosol particles. This feedback can be added to the direct radiative effect of contrails. This would probably increase the climate impact from contrails. Ponater et al. (2002) proposed an approach to parameterize contrails in GCMs that is to make use of a simulated background distribution of aerosols to include details of the nucleation process; this accounts for the aviation effect on cirrus formation due to an accumulation of aircraft emitted aerosols in the upper troposphere. However, this is dependent on an adequate description of the aerosol-cirrus interaction in GCMs that is currently lacking.

(a)

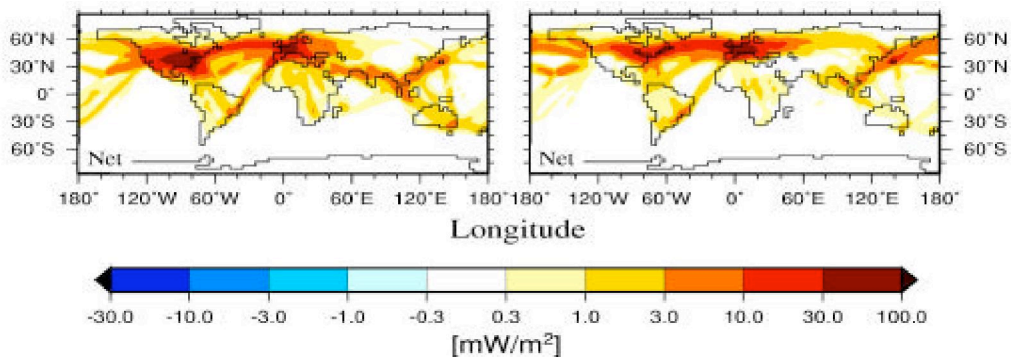

(b)

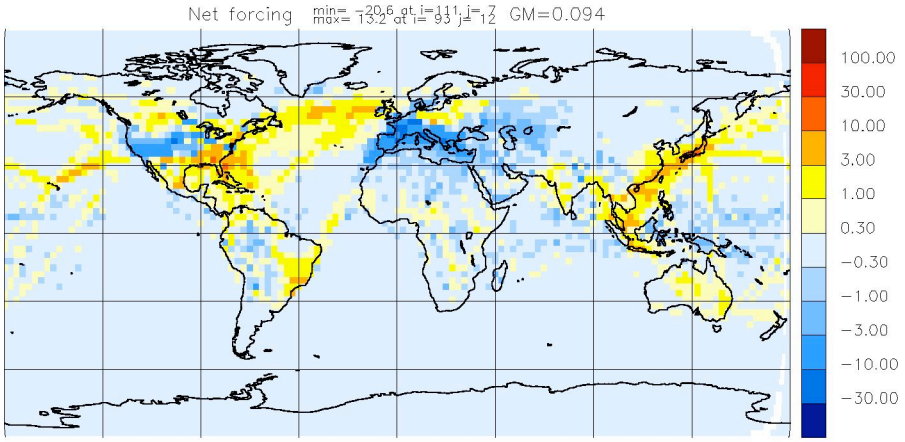

Figure 32. The net radiative forcing of contrails at the top of atmosphere in January (left panel) and July (right panel) from (a) ECHAM4 simulations. Adapted from Marquart et al. (2003) and (b) IFSHAM simulation. Adapated from Guldberg (2003).

3.2.10. Effect of water vapor and temperature on contrails

Atmospheric water vapor is the most important and efficient greenhouse gas (Held and Soden, 2000). It is transparent to incoming short-wave radiation from the Sun and opaque to long-wave radiation leaving the Earth. In general, an increase in atmospheric temperature is accompanied by an increase in water vapor concentration (e.g, Soden et al., 2002; Minschwaner and Dessler, 2004; Soden et al., 2005; Sherwood and Meyer, 2006), leading to further warming. This positive feedback between atmospheric temperature and water vapor is of crucial importance (IPCC, 2007; Randall et al., 2007). Besides the direct effect of water vapor on the earth radiation balance, water vapor also connects to the cloud feedback through its obvious influence on cloud formation.

Recent work on the water budget over the past decade has shown that the water mixing ratio can be understood almost entirely by advection of vapor by the large-scale atmospheric flow combined with removal of water vapor when the relative humidity exceeds 100% (Sherwood, 1996, Salathe and Hartmann, 1997; Dessler and Sherwood,

2000; Dessler and Minschwaner, 2007; Pierrehumbert et al., 2007).

For cloud formation, relative humidity (RH) is the relevant parameter, rather than water vapor mixing ratio. RH connects to mixing ratio through the temperature, so temperature is therefore also a crucial parameter. An important requirement for long-lived contrails is the ice supersaturation, meaning RH > 100%. Thus, accurate knowledge of ice supersaturation is crucial for quantifying both the direct and indirect effects of aviation on cirrus formation. Measurements have recently come on-line that provide some insight into the distribution of supersaturation (Gettelman et al., 2006). They found that supersaturation occurs in humid regions of the upper tropical tropopause near convection 10%-20% of the time at 200 hPa. Supersaturation is very frequent in the extratropical upper troposphere, occurring 20%-40% of the time, and over 50% of the time in storm track regions below the tropopause.

Some efforts have been initiated to take supersaturation into account (Tompkins et al., 2007) in some models such as ECMWF and European Center/Hamburg General Circulation Model (ECHAM). Tomkins et al. (2007) showed the different schemes of the evolution of relative humidity (RH) in an upper-troposphere parcel of air (Figure 33). Figure 33a shows the scheme from Lohmann and Kärcher (2002). It assumes that RH increases with adiabatic cooling until a critical threshold RHcrit which can significantly exceed 100%. At RHcrit, ice crystals are homogeneously nucleated and their uptake of the water vapor reduces towards a value that in most cases just exceeds the 100% level.

Figure 33b shows the scheme assuming any excess humidity is instantaneously converted to ice when RH exceeds 100%. Figure 33c shows the new parameterization developed by Tomkins et al. (2007). This scheme allows supersaturation to occur and converts all humidity exceeding the saturation value to ice instantaneously once the nucleation threshold is attained. The different schemes can result in differences in high-cloud cover and upper tropopause moisture (Tomkins et al., 2007). Clearly, a better understanding of ice supersaturation is crucial for quantifying both direct and indirect effects of aviation on cirrus cloudiness.

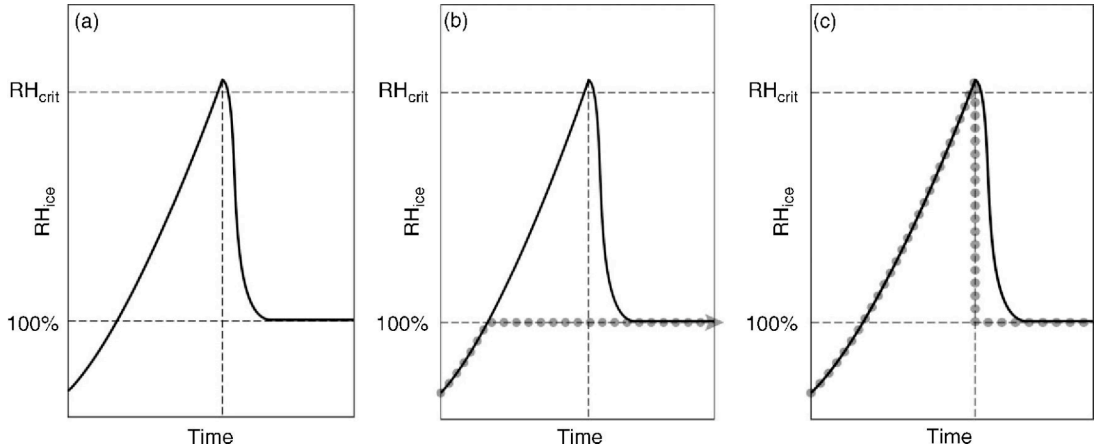

Figure 33. (a) Schematic of evolution of RH in a hypothetical parcel subjext to adiabatic cooling (Lohmann and Kärcher, 2002); (b) the dotted line is the scheme assuming that any excess humidity is instantaneously converted to ice once the RH exceeds 100%; (c) the dotted line is the

scheme assuming that supersaturation to occur and convert all humidity exceeding the saturation value to ice instantaneously once the nucleation threshold is attained (Tomkins et al., 2007).

The dependence of contrail formation on temperature has also long been recognized. Appleman (1953) described the basic theory of contrail formation. The critical temperatures for contrail formation and persistence of contrails and contrail-induced cirrus clouds have been extensively studied (e.g., Coleman, 1996; Schumann, 1996; Schrader, 1997; Jensen et al., 1998). Jensen et al. (1998) investigated the threshold temperatures based on Appleman (1953) theory versus ambient pressure for ambient RH (Figure 34). The observed threshold temperatures were compared by Jensen et al. (1998) with theoretical estimates based on simple models of plume evolution. They found that saturation with respect to liquid water must be reached at some point in the plume evolution. The formation of contrails is needed to further investigate when temperature between liquid-saturation threshold temperature and ice-saturation threshold temperature.

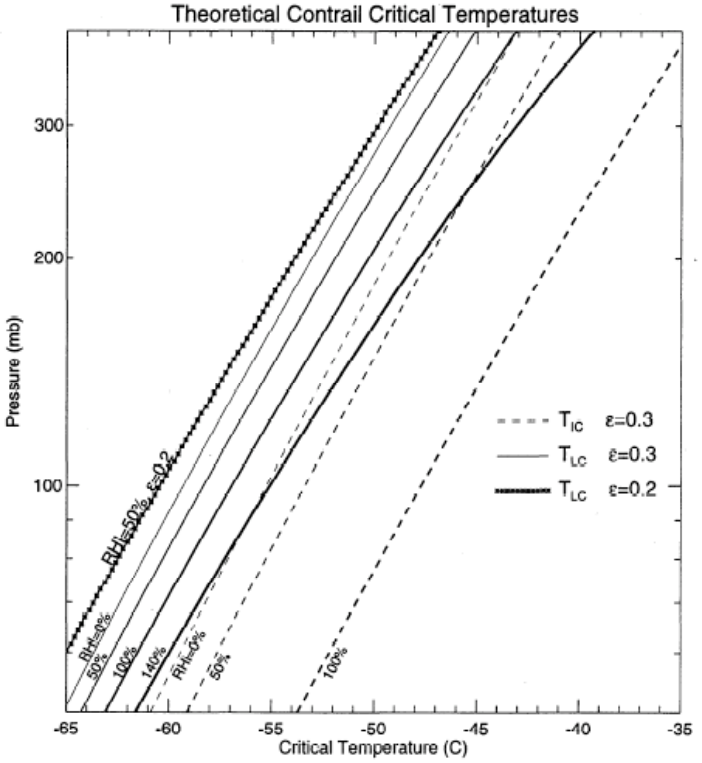

Figure 34. Theoretical threshold temperatures from Appleman (1953) as a function of ambient pressure and RHIs of 0, 50, 100, and 140%. Contrail formation is predicted occur when the ambient temperature is to the left of the solid curves that are for liquid saturation. Dashed curves are for ice saturation. Adapted from Jensen et al. (1998).

The ice-nucleating ability of soot particles in upper troposphere and low stratosphere is also influenced by the environment. The heterogeneous ice nucleation on soot aerosol was investigated at temperatures between 184 and 240 K by Möhler et al. (2003). Figure 35 shows the ice saturation ratios measured for ice nucleation on pure soot and soot coated with sulphuric acid (SA) and ammonium sulphate (AS). The results from DeMoot et al. (1999) are also shown in the figure for comparison to the Aerosol

Interaction and Dynamics in the Atmosphere (AIDA) data (Möhler and Krämer, 2003). At temperatures above 235 K, ice nucleation on pure soot particles only occurred close to or slightly above water saturation (dashed line in Figure 35). When temperatures become lower, ice is formed below both the liquid water saturation threshold and the threshold for homogeneous freezing nucleation of supercooled liquid solution droplets (solid line in Figure 35, Koop et al. 2000). The freezing relative humidity increases 10-20% for the soot particles coated with sulphuric acid (10% mass). These results for the soot particles coated with sulphuric acid from Möhler et al. (2003) is in contrast to those results present by DeMott et al. (1999) showing that increasing amount of sulphuric acid coating decreases freezing relative humidity.

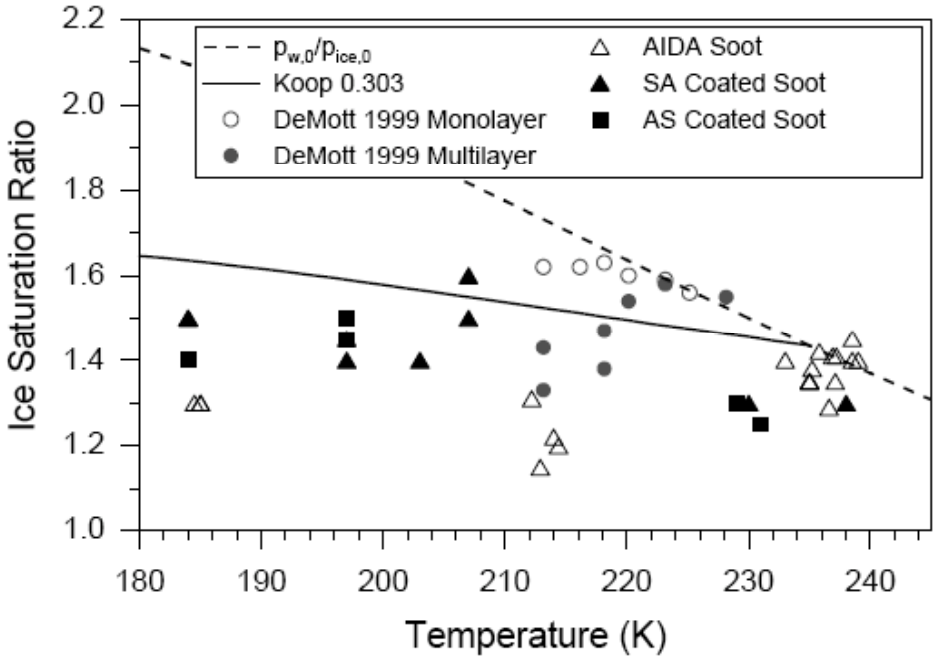

Figure 35. The ice saturation ratios measured for ice nucleation on pure soot and soot coated with sulphuri acid (SA) and ammonium sulphate (AS). The results from DeMoot et al. (1999) are also shown in the figure for comparison to the Aerosol Interaction and Dynamics in the Atmosphere (AIDA) data (Möhler et al. 2003).

4. Prioritization of Outstanding Issues

4.1 Prioritized areas

4.1.1. Single-scattering Properties of Particles in Contrails and Contrail-induced Cirrus Clouds

An extensive database of single-scatting properties of ice particles has been built by Yang et al. (2000, 2005) and Baum et al. (2005a, b, c). The habits for droxtals, hollow and solid columns, 3D bullet rosettes (with solid bullets), plates, and aggregates have all been calculated. Further work is ongoing with regards to a new particle: a 3D bullet rosette that has hollow bullets. Inclusions at the ends of the individual bullets are more

realistic, and these particles have very different scattering properties than those obtained for the solid bullet rosettes. At present, there is no suitable database for aerosols and ice particles in contrails and contrail-induced cirrus clouds. As a result, the studies on the radiative forcing of contrails and contrail-induced cirrus clouds use scattering properties of either spherical ice particles or of nonspherical ice particles whose optical properties are calculated theoretically. A database of single-scattering properties for specified (more realistic) particle habits in contrails and contrail-induced cirrus clouds will reduce the uncertainties of radiative forcing of contrails and contrail-induced cirrus clouds. These databases are also the basis for the parameterization of radiation from contrails and contrail-induced cirrus clouds for use in GCMs.

As mentioned in the section "present state of modeling capability/best approach for light scattering computation", the most practical approach is a combination of FDTD, DDA, T-matrix methods and the ray-tracing technique. The limitations and gaps of this combination scheme need to be resolved. First, the applicability of geometric optics to light scattering is not clear. Generally, it is believed that geometric optics will produce reasonable results when the particle is very large compared with the wavelength. But in some special cases, the result obtained using geometric optics is wrong. Take an oriented plate as an example; the extinction efficiency is not going to converge to 2 even for a particle with a very large size. This phenomenon is due to missing the edge effect in this method. Because the particle is very large, it is also impossible to use DDA to include the edge effects. Second, there are still no ray-tracing codes to make a "educated guess" of the internal field within an ice crystal. The efficiency of the combination of DDA and the ray-tracing method to include the edge effect is still unknown. The answer to this question needs both theoretical and numerical analyses.

4.1.2. Parameterization of Radiation Forcing of Contrails and Contrail-induced Cirrus Clouds for Use in GCMs

The radiative forcing of contrails and contrail-induced cirrus clouds in GCMs is based on the shortwave and longwave radiation schemes used for natural cirrus clouds. Building new parameterization schemes suitable for contrails and contrail-induced cirrus clouds will bring more accurate estimates of radiative forcing of these clouds. This also provides an efficient way to understand the differences in the radiative forcing from contrails, contrail-induced cirrus clouds, and natural cirrus clouds.

4.1.3 Detecting Contrails and Contrail-induced Cirrus Clouds from Multi Satellite Measurements

The detection of cloud properties is sensitive to the satellite sensors and the retrieval algorithms used (Wielicki and Parker, 1992; Hong et al., 2007b). The satellites in the A-Train include passive visible and infrared sensors (MODIS aboard Aqua), active lidar (CALIPSO), and passive polarization measurements (POLDER). These sensors provide a wealth of measurements to study the properties of contrails and contrail-induced cirrus

clouds that could reduce the uncertainties in the radiative forcing of contrails and contrail-induced cirrus clouds.

4.1.4 Understanding Formation of Contrails and Contrail-induced Cirrus Clouds

A better understanding of the formation mechanisms of contrails and contrail-induced cirrus clouds will improve the representation of these clouds in GCMs. Important factors for contrail formation include both water vapor and temperature, which combine to determine relative humidity. It is also necessary to further investigate the liquid-saturation threshold temperature and ice-saturation threshold temperature for contrail formation. At present, only a handful of climate models allow supersaturation.

4.1.5. Interaction Between Aerosols and Cirrus Clouds

Theoretical modeling of the coupling between direct and indirect aviation effects on high clouds is currently very rudimentary (Kärcher et al., 2007). Further modeling, in situ measurements, and laboratory experiments are needed to improve our understanding of this important interaction. This effort will also improve the knowledge of the transition of contrails into cirrus clouds.

4.2 Estimated costs and timelines for prioritized areas

As stated previously, we have identified five prioritized research topics that are critical to a better understanding the optical and radiative forcing of contrails and contrail-cirrus clouds:

Topic 1. Development of reliable data sets for the optical properties of individual ice crystals with various shapes and sizes, typical in contrails and contrail-cirrus clouds. The data sets will be developed for both the solar and thermal infrared spectra with an adequate spectral resolution. This effort will be based mainly on numerical simulation. However, laboratory and in-situ measurements are required to validate the theoretical simulation.

Topic 2. Parameterization of the radiative properties of contrails and contrail-cirrus clouds for applications to climate models. The single-scattering data sets developed in Topic 1 for individual ice crystals need to be merged with in-situ measured particle size distributions and habit mixtures. The resultant bulk optical properties need to be parameterized as functions of particle effective size. Furthermore, the parameterization needs to be incorporated into the radiative transfer schemes involved in climate models. The validation of the parameterization based on spaceborne and ground-based radiometric measurements is necessary.

Topic3. Detection of contrails and contrail-cirrus clouds from synergetic use of the measurements made by multiple satellite sensors. To understand the

radiative forcing of contrails and contrail-cirrus clouds from a global perspective, it is necessary to detect contrails and contrail-cirrus clouds. New techniques using various spectral bands need to be developed to effectively identify contrails and contrail-cirrus in satellite images.

Topic 4. Understanding of the formation of contrails and contrail-induced cirrus clouds. To fully understand the radiative forcing of contrails and contrail-induced cirrus clouds, it is necessary to understand the impact of ambient atmospheric environments on these clouds, which requires an improved knowledge about the formation of contrails and contrail-induced cirrus clouds. The most important factors for contrail formation are water vapor and temperature as discussed in section 3.2.10

Topic 5. Interaction between aerosols and contrails/contrail-cirrus clouds. To understand the indirect radiative effect of contrails/contrail-cirrus clouds, it is necessary to understand the interaction of aerosols and contrails/contrail-cirrus clouds. This is a very broad research area and requires tremendous efforts.

Table 1 lists the estimated costs and timeline for the aforementioned five prioritized research topics.

Table 1. Prioritized areas, estimated costs, and timeline.

Prioritized areas	# of FTE	Duration of Efforts
Topic 1	2	3 years
Topic 2	2	2.5 years
Topic 3	3	3 years
Topic 4	3	3 years
Topic 5	4	3 years

5. Recommendations for best use of current tools for modeling and data analysis

Topic-specific recommendations for the five topics listed in Sec. 4 are as follows:

•A combination of the FDTD (or DDA) and geometric optics method (GOM) is recommended. The FDTD and DDA are accurate methods, but their applications are limited to small ice crystals because of tremendous computational demand of these methods. The GOM is approximate method that is valid for large ice crystals. This approach has been proven quite successful for applications to ice crystals in natural cirrus clouds. Because ice crystals in contrails and contrail-cirrus clouds are relatively smaller than naturally occuring cirrus clouds, it is critical to ensure an adequate bridging the FDTD (or DDA) solutions and the GOM solutions.

•The parameterization needs to be done for radiative transfer schemes used in several popular climate models such as the NCAR Community Atmosphere Model (CAM). The validation of the parameterization can be carried out by comparing the model simulations of radiation fluxes and their measurement counterparts (e.g., the CERES data and DOE-ARM ground radiometric measurements).

•New efforts are recommended to explore the spectral, viewing-geometry, and polarization characteristics of several existing satellite sensors (e.g., MODIS, AIRS, MISR, and POLDER) to effectively detect contrails and contrail-cirrus clouds. Some channels (e.g., the MODIS band 26 centered at 1.37 μm) have proved effective in detecting high clouds.

•More in-situ observations regarding the relationship between contrails and ambient parameters are recommended. Recently, the ECWMF, ECHAM4, and IFSHAM models from Europe have included the capabilities of predicting the supersaturation. Thus, in addition to in situ measurements, modeling is also an efficient way to understand the influence of water vapor and temperature on contrail formation.

• The interaction between aerosols and contrails/contrail-cirrus clouds is a quite open research area. In addition to in-situ measurements of the correlation of aerosols and contrails, cloud models may play an important role to accomplish this research task.

References:

Appleman, H., 1953: The formation of exhaust condensation trails by jet aircraft, *Bull. Amer. Meteor. Soc., 34,* 14–20.

Atlas, D., Z. Wang, D. Duda, 2006: Contrails to Cirrus – Morphology, Microphysics, and Radiative Properties. *J. Appl. Meteor. Climatol., 45,* 5–19.

Bacon, N. J. and B. D. Swanson, 2000: Laboratory Measurements of Light Scattering by Single Levitated Ice Crystals Neil J. Bacon and Brian D. Swanson, *J. Atmos. Sci. 57 2094-2104*

Bacon, N. J., B. D. Swanson, M. B. Baker, and E. J. Davis, 1998: Laboratory Measurements of Light Scattering by Single Ice Particles Neil J. Bacon, Brian D. Swanson, Marcia B. Baker and E. James Davis, *J. Aerosol Sci. Vol. 29, S1317--S1318.*

Bakan, S., M. Betancor, V. Gayler, and H. Grassl, 1994: Contrail frequency over Europe from NOAA-satellite images. *Ann. Geophys., 12,* 962–968.

Barkey, B., K.N. Liou, Y. Takano, and W. Gellermann, 2000: Experimental and theoretical spectral reflection measurements of ice clouds generated in a laboratory chamber. *Appl. Opt.*, 39, 3561-3564.

Baum, B. A., A. J. Heymsfield, P. Yang, S. T. Bedka (2005a), Bulk scattering properties for the remote sensing of ice clouds. Part I: Microphysical data and models. *J. Appl. Meteorol., 44,* 1885–1895.

Baum, B. A., P. Yang, A. J. Heymsfield, S. Platnick, M. D. King, Y.-X. Hu, and S. T. Bedka (2005b), Bulk scattering properties for the remote sensing of ice clouds, Part II: Narrowband Models. *J. Appl. Meteorol., 44,* 1896–1911.

Baum, B. A., P. Yang, S. L. Nasiri, A. K. Heidinger, A. J. Heymsfield, and J. Li (2007), Bulk scattering properties for the remote sensing of ice clouds. Part III: High resolution spectral models from 100 to 3250 cm-1, *J. Appl. Meteor. Clim., 46,* 423–434.

Boucher, O., 1999: Air traffic may increase cirrus cloudiness. *Nature, 397,* 30–31.

Broecher, W., Lecture presented AGU 1996 – Baltimore US. 1996, Lamont-Doherty Earth Observatory, Columbia University.

Cai, Q., and K. N. Liou, 1982: Polarized light scattering by hexagonal ice crystals: Theory. *Appl. Opt.* **21**, 3569-3580.

Chylek, P. and J. Hallett, 1992: Enhanced absorption of solar radiation by cloud droplets containing soot particles in their surface. *Q. J. R. Meteor. Soc., 118,* 167–172.

Clough, S. A., M. J. Iacono, and J.-L. Moncet, 1992: Line-by-line calculations of atmospheric fluxes and cooling rates: Application to water vapor, *J. Geophys. Res., 97,* 15,761-15, 785.

Coleman, R. F., 1996: a new formulation for the critical temperature for contrail formation, *J. Appl. Meteorol., 35,* 2270-2282.

DeMott, P. J., Y. Chen, S. M. Kreidenweis, D. C. Rogers, and D. E. Sherman, 1999: Ice formation by black carbon particles. *Geophys. Res. Lett.,* 26, 2429-2432.

Dessler, A. E., and K. Minschwaner, 2007: An analysis of the regulation of tropical tropospheric water vapor, *J. Geophys. Res., 112,* DOI: 10.1029/2006JD007683.

Dessler, A. E., and S. C. Sherwood, 2000: Simulations of tropical upper tropospheric humidity, *J. Geophys. Res., 105,* 20,155–20,163.

Draine, B. T., and P. J. Flatau, 1994: Discrete-dipole approximation for scattering calculations. *J. Opt. Soc. Am. A* **11**, 1491-1499.

Duda, D. P., and J. D. Spinhirne,1996: Split-window retrieval of particle size and optical depth in contrails located above horizontal inhomogeneous ice clouds. *Geophys. Res. Lett., 23,* 3711–3714.

Duda, D. P., J. D. Spinhirne, and W. D. Hart, 1998: Retrieval of contrail microphysical properties during SUCCESS by the split-window method. *Geophys. Res. Lett., 25,* 1149–1152.

Duda, D. P., P. Minnis, P. K. Costulis, R. Palikonda, 2003: CONUS Contrail Frequency Estimated from RUC and Flight Track Data. European Conference on Aviation, Atmosphere, and Climate.

Duda, D. P., P. Minnis, and L. Nguyen, 2001: Estimates of cloud radiative forcing in contrail clusters using GOES imagery. *J. Geophys. Res., 106,* 4927–4937.

Duda, D. P., P. Minnis, L. Nguyen, and R. Palikonda, 2004: A case study of the development of contrail clusters over the Great Lakes. *J. Atmos. Sci., 61,* 1132–1146.

Fahey, D. W., U. Schumann, S. Ackerman, P. Artaxo, O. Boucher, M.Y. Danilin, B. Kärcher, P. Minnis, T. Nakajima, and O.B. Toon, 1999: Aviation-produced aerosols and cloudiness. In Aviation and the Global Atmosphere, J. E. Penner, D. H. Lister, D. J. Griggs, D. J. Dokken, and M. McFarland (Eds.), Cambridge University Press, Cambridge, U.K., 65–120.

Fichter, C., S. Marquar, R. Sausen, and D. S. Lee, 2005: The impact of cruise altitude on contrails and related radiative forcing. *Meteorol. Zeitschrift, 14,* 14,563–14,572.

Foot, J. S., 1988: Some observations of the optical properties of clouds, II, Cirrus. *Q. J. R. Meteorol. Soc.*, 114, 145-164.

Fu, Q., and K.-N. Liou, 1993: Parameterization of the radiative properties of cirrus clouds. *J. Atmos. Sci., 50,* 2008–2025.

Frey, R., B. Baum, W. Menzel, S. Ackerman, C. Moeller, and J. Spinhirne, 1999: A comparison of cloud top heights computed from airborne lidar and MAS radiance data using CO2 slicing. *J. Geophy. Res., 104,* 10.1029/1999JD900796.

Gao, B.-C., A. F. H. Goetz, and W. J. Wiscombe, 1993: Cirrus cloud detection from airborne imaging spectrometer data using the 1.38 μm water vapor band. *Geophys. Res. Lett., 20,* 301–304.

Gao, B.-C., Y. J. Kaufman, W. Han, and W. J. Wiscombe, 1998: Correction of thin cirrus path radiance in the 0.4–1.0 μm spectral region using the sensitive 1.375 μm cirrus detecting channel. *J. Geophys. Res., 103,* 32,169–32,176.

Gao, B.-C., K. Meyer, and P. Yang, 2004: A new concept on remote sensing of cirrus optical depth and effective ice particle size using strong water vapor absorption channels near 1.38 and 1.88 μm. *IEEE Trans. Geosci. Remote Sens., 42,* 1891–1899.

Garrett, T. J., 2007: Comments on "Effective radius of ice cloud particle populations derived from aircraft probes". *J. Atmos. Oceanic. Technol. 24,* 1492–1503.

Garrett T. J., H. Gerber, D. G. Baumgardner, C. H. Twohy, and E. M. Weinstock, 2003: Small, highly reflective ice crystals in low-latitude cirrus. *Geophys. Res. Lett., 30,* doi:10.1029/2003GL018153.

Gayet. J.-F., G. Febvre, G, Brogniez, H. Chepfer, W. Renger, and P. Wendling, 1996: Microphysical and optical properties of cirrus and contrails: Cloud field study on 13 October 1989. *J. Atmos. Sci., 53,* 126–138.

Gettelman, A., E. J. Fetzer, A. Eldering, and F. W. Irion, 2006: The global distribution of supersaturation in the upper troposphere from the Atmospheric Infrared Sounder, *J. Climate, 19,* 6089–6103.

Goodman, J., R. F. Pueschel, E. J. Jensen, S. Yerma, G. V. Ferr y, S. D. Howard, S. A. Kinne, and D. Baumgardner, 1998: Shape and size of contrails ice particles. *Geophys. Res. Lett., 25,* 1327–1330.

Gothe, M. B., and H. Grassl, 1993: Satellite remote sensing of the optical depth and mean crystal size of thin cirrus and contrails. *Theor. Appl. Climatol., 48,* 101–113.

Guldberg, A., 2003: A study of contrails in a General Circulation Model, proceeding of the AAC-Conference, June 30 to July 3, 2003, Friedrichshafen, Germany, 261–265.

Haywood, J. M., and K.P. Shine, 1997: The effect of anthropogenic sulfate and soot aerosol on the clear sky planetary radiation budget. *Geophy. Res. Lett., 22,* 603–606.

Hess, M., and Wiegner, M., 1994: COP: a data library of optical properties of hexagonal ice crystals. *Appl. Opt. 33,* 7740-7746.

Held, I. M., and B. J. Soden, 2000: Water vapor feedback and global warming, *Ann. Rev. Energy Environ., 25,* 441–475.

Heymsfield A. J., C. Schmitt, A. Bansemer, G.-J. Van Zadelhoff, M. J. McGill, C. Twohy, D. Baumgardner, 2006: Effective Radius of Ice Cloud Particle Populations Derived from Aircraft Probes. *J. Atmos. Ocean. Technol., 23,* 361–380.

Hong, G., P. Yang, H.-L. Huang, B. A. Baum, Y. X. Hu, and S. Platnick, 2007a: The sensitivity of ice cloud optical and microphysical passive satellite retrievals to cloud geometrical thickness. *IEEE Trans Geosci. Remote Sens., 45,* 1315–1323.

Hong, G., P. Yang, B.-C. Gao, B. A. Baum, Y. X. Hu, M. D. King, and S. Platnick, 2007b: High cloud properties from three years of MODIS Terra and Aqua data over the Tropics. *J. Appl. Meteor. Climatol., 46,* 1840–1856.

Immler F., and O. Schrems, 2003:Comparison of cirrus cloud properties in the northern and southern hemisphere on the basis of lidar measurements. European Conference on Aviation, Atmosphere, and Climate.

Immler, F., R. Treffeisen, D. Engelbart, K. Krüger, and O. Schrems, 2007: Cirrus, contrails, and ice supersaturated regions in high pressure systems at northern mid latitudes. *Atmos. Chem. Phys. Discuss., 7,* 13,175–13,201.

Minschwaner, K., and A. E. Dessler, 2004: Water vapor feedback in the tropical upper troposphere: Model results and observations, *J. Climate, 17,* 1272–1282.

Möhler, O, and C. Linke, H. Saathoff, M. Schnaiter, R. Wagner, U. Schurath, A. Mangold, M. Krämer, 2003: Experimental investigation of homogeneous and heterogeneous freezing processes at simulated UTLS conditions. European Conference on Aviation, Atmosphere, and Climate.

Jacobowitz, H., 1971: A method for computing the transfer of solar radiation through clouds of hexagonal ice crystals. J. Quant. Spectrosc. Radiat. Transfer 11, 691–695.

Jensen, E.J., A.S. Ackerman, D.E. Stevens, O.B. Toon, and P. Minnis, 1998: Spreading and growth of contrails in a sheared environment. *J. Geophys. Res., 103,* 31,557–31,568, doi:10.1029/98JD02594.

Jensen, E. J., O. B. Toon, S. Kinne, G. W. Sachse, B. E. Anderson, K. R. Chan, C. H. Twohy, B. Gandrud, A. Heymsfield, and R. C. Miake-Lye, 1998: Environmental conditions required for contrail formation and persistence, *J. Geophys. Res., 103,* 3929–3936.

Jones, R. L., and J. F. B. Mitchell, 1991, Is water vapour understood? Nature, 353, 210.

Kärcher, B., O. Möhler, P. J. DeMott, S. Pechtl, and F. Yu, 2007: Atmospheric Chemistry and Physics Insights into the role of soot aerosols in cirrus cloud formation. *Atmos. Chem. Phys., 7,* 4203–4227.

Kärcher, B., and J. Ström, 2003: The roles of dynamical variability and aerosols in cirrus cloud formation. *Atmos. Chem. Phys., 3,* 823–838.

Karl T. R., and K. E. Trenberth, 2003: Modern global climate change. Science, 302, 1719–1723.

King, M. D., S. Platnick, P. Yang, G. T. Arnold, M. A. Gray, J. C.Riédi, S. A. Ackerman, and K. N. Liou, 2004: Remote sensing of liquid water and ice cloud optical thickness, and effective radius in the arctic: Application of airborne multispectral MAS data, *J. Atmos. and Ocean. Technol., 21,* 857–875.

Koop, T., B. P. Luo, A. Tsias, and T. Peter, 2000: Water activity as the determinant for homogeneous ice nucleation in aqueous solutions. *Nature,* 406, 611-614.

Kuhn, M., A. Petzold, D. Baumgardner, and F. Schröder, 1998: Particle composition of a young condensation trail and of upper tropospheric aerosol. *Geophys. Res. Lett., 25,* 2679–2682.

Liou, K. N., Y. Takano , S. C. Ou , A. Heymsfield , and W. Kreiss, 1990: Infrared transmission through cirrus clouds: a radiative model for target detection. *Appl. Opt., 29,* 1886–1896.

Liou, K.N., Y. Takano, and P. Yang, 2000: Light scattering and radiative transfer in ice crystal clouds: Applications to climate research. In "Light Scattering by Nonspherical Particles: Theory, Measurements and Geophysical Applications." Eds. M.I. Mishchenko, J.W. Hovenier, and L.D. Travis, Academic Press, New York, Chapter 15.

Liou, K.N., P. Yang, Y. Takano, K. Sassen, T.P. Charlock, and W.P. Arnott, 1998: On the radiative properties of contrail cirrus. *Geophys. Res. Lett., 25,* 1161–1164.

Lohmann, U., and B. Kärcher, 2002: First interactive simulations of cirrus clouds formed by homogeneous freezing in the ECHAM GCM. *J. Geophys. Res., 107(D10), 4105,* doi:10.1029/2001JD000767.

Macke, A., 1993: Scattering of light by polyhedral ice crystals. *Appl. Opt.* **32**, 2780-2788.

Macke, A. J. Mueller, and E. Raschke, 1996: Single scattering properties of atmospheric ice crystal. *J. Atmos. Sci.* **53**, 2813-2825.

Mangold, A., R. Wagner, H. Saathoff, U. Schurath, C. Giesemann, V. Ebert, M. Krämer, and O. Möhler, 2005: Experimental investigation of ice nucleation by different types of aerosols in the aerosol chamber AIDA: implications to microphysics of cirrus clouds. *Meteorol. Z., 14,* 485–497.

Mannstein, H., R. Meyer, and P. Wendling, 1999: Operational detection of contrails from NOAAAVHRR-data. *Int. J. Remote Sensing, 20,* 1641–1660.

Marquart, S., M, Ponater, F. Mager, and R. Sausen, 2003: Future development of contrails: Impacts of increasing air traffic and climate change, proceeding of the AAC-Conference, June 30 to July 3, 2003, Friedrichshafen, Germany, 255–260.

Marquart, S., M. Ponater, F. Mager, and R. Sausen, 2003: Future development of contrail cover, optical depth, and radiative forcing: Impacts of Increasing Air Traffic and Climate Change. *J. Climate, 16,* 2890–2904.

Meerkötter, R., U. Schumann, D. R. Doelling, P. Minnis, T. Nakajima, and Y. Tsushima, 1999: Radiative forcing by contrails. Ann. Geophys., 17, 1070–1084.

Meyer, R., H. Mannstein, R. Meerkötter, U. Schumann, and P. Wendling, 2002: Regional radiative forcing by line-shaped contrails derived from satellite data. *J. Geophys. Res., 107(D10), 4104,* doi:10.1029/2001JD000426.

Minnis, P., J.K. Ayers, R. Palikonda, E. Phan, 2004: Contrails, Cirrus Trends, and Climate. *J. Climate, 17,* 1671–1685.

Minnis, P., U. Schumann, D. R. Doelling, K. Gierens, and D. Fahey, 1999: Global distribution of contrail radiative forcing. *Geophys. Res. Lett., 26,* 1853–1856.

Minnis, P., L. Nguyen, D. P. Duda, and R. Palikonda, 2002: Spreading of isolated controls during the 2001 air traffic shutdown. Preprints, 10th Conf. on Aviation, Range, and Aerospace Meteorology, Portland, OR, Amer. Meteor. Soc., J9–J12.

Minnis, P., D. F. Young, L. Nguyen, D. P. Garber, W. L. Smith, Jr., and R. Palikonda, 1998: Transformation of contrails into cirrus during SUCCESS. *Geophys. Res. Lett., 25,* 1157–1160.

Mishchenko, M. I., and L. D. Travis, 1994: Light scattering by polydispersions of randomly oriented spheroids with sizes comparable to wavelengths of observation, *Appl. Opt., 33,* 7206-7225.

Mishchenko, M. I., and K. Sassen, 1998: Depolarization of lidar returns by small ice crystals: an application to contrails, *Geophys. Res. Lett., 25,* 309-312.

Mishchenko, M. I., L. D. Travis, and A. Macke, 2000: *T*-matrix method and its applications. In *Light Scattering by Nonspherical Particles: Theory, Measurements, and Applications* (M. I. Mishchenko, L. D. Travis, and J. W. Hovenier, Eds.), Academic Press, San Diego, pp. 147-172.

Myhre, G., and F. Stordal, 2001: Global sensitivity experiments of the radiative forcing due to mineral aerosols. *J. Geophys. Res., 106,* 18,193–18,204.

Muinonen, K., 1989: Scattering of light by crystals: a modified Kirchhoff approximation. *Appl. Opt., 28,* 3044-3050.

Noel, V., D. M. Winker, T. J. Garrett, and M. McGill, 2007: Extinction coefficients retrieved in deep tropical ice clouds from lidar observations using a CALIPSO-like algorithm compared to in-situ measurements from the cloud integrating nephelometer during CRYSTAL-FACE. Atmos. Chem. Phys., 7, 1415–1422.

Palikonda, R., D. N. Phan, V. Chakrapani, and P. Minnis, 2004: Contrail coverage over the USA from MODIS and AVHRR data. Preprints, European Conf. on Aviation, Atmosphere, and Climate, Friedrichshafen at Lake Constance, Germany, Institut fu¨ r Physik der Atmospha¨re, DLR, in press. [Available online at http://www-pm.larc.nasa.gov/sass/pub/conference/rabi.AAC.03.pdf.]

Parol, F., J. C. Buriez, G. Brogniez, and Y. Fouquart, 1991: Information content of AVHRR channels 4 and 5 with respect to the effective radius of cirrus cloud particles. *J. Appl. Meteor., 24,* 973–984.

Petzold, A., and Coauthors, 1997: Near field measurements on contrail properties from fuels with different sulfur content. *J. Geophys. Res., 102,* 29,867–29,880.

Petzold, A., A. Döpelheuer, C. A. Brock, and F. Schröder, 1999: In situ observations and model calculations of black carbon emission by aircraft at cruise altitude. *J. Geophys. Res., 104,* 22 171–22 181.

Pierrehumbert, R. T., H. Brogniez, and R. Roca, 2007: On the relative humidity of the Earth's atmosphere, in The Global Circulation of the Atmosphere, Schneider, T., and A. H. Sobel (eds.), Princeton Univ. Press.

Ponater, M., S. Brinkop, R. Sausen, U. Schumann, 1996: Simulating the global atmospheric response to aircraft water vapor emission and contrails: a first approach using a GCM. *Annales De Geophysique, 14,* 941–960.

Ponater, M., S. Marquart, and R. Sausen, 2002: Contrails in a comprehensive global climate model: parameterisation and radiative forcing results. *J. Geophys. Res., 107,* 10.1029/2001JD000429.

Prabhakara, C., R. S. Fraser, G. Dalu, M. L. C. Wu, R. J. Curran, and T. Styles, 1988: Thin cirrus clouds: Seasonal distribution over oceans deduced from Nimbus-4 IRIS. *J. Appl. Meteor., 27,* 379–399.

Purcell, E. M. and C. R. Pennypacker, 1973: Scattering and absorption of light by nonspherical dielectric grains. *Astrophys. J. 186,* 705-714.

Ramanathan, V., R. D. Cess, E. F. Harrison, P. Minnis, B. R. Barkstrom, E. Ahmad, and D. Hartmann, 1989: Cloud radiative forcing and climate: Results from the ERBE, *Science, 243,* 57–63.

Randall et al., 2007: Cilmate Models and Their Evaluation. In: Climate Change 2007: The Physical Science Basis. Contribution of Working Group I to the Fourth Assessment Report of the Intergovernmental Panel on Climate Change, Solomon, S., D. Qin, M. Manning, Z. Chen, M. Marquis, K. B. Averyt, M. Tignor and H. L. Miller (eds.), Cambridge University Press, Cambridge, United Kingdom and New York, NY, USA.

Rädel, G., C. J. Stubenrauch, R. Holz, and D. L. Mitchell, 2003: Retrieval of effective ice crystal size in the infrared: Sensitivity study and global measurements from the TIROS-N Operational Vertical Sounder. *J. Geophys. Res., 108,* 4281–4292.

Rind, D., P. Lonergan, and K. Shah, 1996: Climatic Effect of water vapor release in the upper troposphere. *J. Geophy. Res., 101,* 29,395–29,405.

Rind, D., P. Lonergan, and K. Shah, 2000: Modeled impact of cirrus cloud increases along aircraft flight paths. *J. Geophy. Res., 105,* 19,297–19,940.

Rossow, W. B., and R. A. Schiffer, "Advances in understanding clouds from ISCCP," *Bull. Am. Meteorol. Soc., 80,* 2261-2287 (1999).

Salathe, E. P., and D. L. Hartmann, 1997: A trajectory analysis of tropical upper-tropospheric moisture and convection, *J. Climate, 10,* 2533–2547.

Sassen, K., 1997: Contrail-cirrus and their potential for regional climate change. *Bull. Amer. Meteor. Soc., 78,* 1885–1903.

Sassen, K., and J. R. Campbell, 2001: A midlatitude cirrus cloud climatology from the Facility for Atmospheric Remote Sensing: I. Macrophysical and synoptic properties. *J. Atmos. Sci., 58,* 481–496.

Sassen, K., and C. Hsueh, 1998: Contrail properties derived from high-resolution polarization lidar studies during SUCCESS. *Geophys. Res. Lett., 25,* 1165–1168.

Sassen, K., and K.N. Liou, 1979a: Scattering of polarized laser light by water droplet, mixed phase, and ice crystal clouds: I. Angular Scattering patterns. *J. Atmos. Sci.*,

36, 838-851.
Sassen, K., and K.N. Liou, 1979b: Scattering of polarized laser light by water droplet, mixed phase and ice crystal clouds: II. Angular depolarizing and multiple scattering behavior. *J. Atmos. Sci.*, 36, 852-861.
Sausen, R., K. Gierens, M. Ponater, and U. Schumann, 1998: A diagnostic study of the global distribution of contrails. Part I: Present day climate. *Theor. Appl. Climatol., 61,* 127–141.
Sausen, R. I. Isaksen, V. Grewe, D. Hauglustaine, D. Lee, G. Myhre, M. Köhler, G. Pitari, U. Schumann, F. Stordal, C. Zerefos, 2005: Aviation radiative forcing in 2000: An update on IPCC (1999). *Meteorologische Zeitschrift, 14-4,* 555–561.
Schmitt, A., Brunner, B., 1997: Emissions from aviation and their development over time. In: Schumann, U., Chlond, A., Ebel, A., KaÈrcher, B., Pak, H., Schlager, H., Schmitt, A., Wendling, P. (eds.) Pollutants from Air Traffic Results of Atmospheric Research 1992-1997. DLR Mitteilung 97-04, 37–52.
Schörder, F.; B. Kärcher, C. Duroure, J. Strm, A. Petzold, J.-F. Gayet, B. Strauss, P. Wendling, S. Borrmann, 2000: On the transition of contrails into cirrus clouds. *J. Atmos. Sci., 57,* 464–480.
Schneider, E. K., B. P. Kirtman, and R. S. Lindzen, 1999: Tropospheric water vapor and climate sensitivity, *J. Atmos. Sci., 36,* 1649–1658.
Schrader, M. L., W. D. Meyer, and C. L. Weaver, 1997: Comments on "A reexamination of the formation of exhaust condensation trails by jet aircraft." *J. Appl. Meteor., 36,* 623–626.
Schumann, U., 1996: On conditions for contrail formation from aircraft exhausts, *Meteor. Z., N.F. 5,* 3–22.
Schumann, U. and P. Wendling, 1990: Determination of contrails from satellite data and observational results. Air traffic and the environment–background, tendencies, and potential global atmospheric effects, Springer–Verlag, Berlin, Heidelberg, New York, USA, 138–153.
Sherwood, S. C., 1996: Maintenance of the free-tropospheric tropical water vapor distribution. Part II: Simulation by large-scale advection, *J. Climate, 9,* 2919–2934.
Sherwood, S. C., and C. L. Meyer, 2006: The general circulation and robust relative humidity, *J. Climate, 19,* 6278–6290.
Shine K. P., and A. Sinha, 1991: Sensitivity of the earth's climate to height dependent changes in the water vapor mixing ratio. Nature, 354, 382–384.
Sinha, A., and J. E. Harris, 1995: Water vapour and greenhouse trapping: the role of far infrared absorption, *Geophys. Res. Lett., 22,* 2147–2150.
Soden, B. J., D. L. Jackson, V. Ramaswamy, M. D. Schwarzkopf, and X. Huang, 2005: The radiative signature of upper tropospheric moistening, *Science, 310,* 841–844.
Soden, B. J., R. T. Wetherald, G. L. Stenchikov, and A. Robok, 2002: Global cooling after the eruption of Mount Pinatubo: A test of climate feedback by water vapor, *Science, 296,* 727–730.
Strauss, B., 1994: Über den Einfluss natürlicher und anthropogener Eiswolken auf das regionale Klima mit besonderer Berücksichtigung des mikrophysikalischen Einflusses. Dtsch. Luft Raumfahrt Forschungsber. 94-23, 97.

Stordal, F., G. Myhre, E. J. G. Stordal, W. B. Rossow, D. S. Lee, D. W. Arlander, and T. Svendby, 2005: Is there a trend in cirrus cloud cover due to aircraft traffic? *Atmos. Chem. Phys., 5,* 2155–2162.

Ström J., and S. Ohlsson, 1998, In situ measurements of enhanced crystal number densities in cirrus clouds caused by aircraft exhaust. *J. Geophys. Res. 103(D10):* 11355–11361.

Stubenrauch, C. J., R. Holz, A. Chédin, D. L. Mitchell, and A. J. Baran, 1999: Retrieval of cirrus ice crystal sizes from 8.3 and 11.1 μm emissivities determined by the improved initialization inversion of TIROS-N Operational Vertical Sounder. *J. Geophys. Res., 104,* 31,793–31,808.

Stuber, N., P. Forster, G. Rädel, and K. Shine, 2006: The importance of the diurnal and annual cycle of air traffic for contrail radiative forcing. *Nature, 441,* 864–867.

Stuber, N., and P. M. Forster, 2007: The impact of diurnal variations of air traffic on contrail radiative forcing. *Atmospheric Chemistry and Physics, 7,* 3153–3162.

Sussmann R., 1997: Optical properties of contrail-induced cirrus: Discussion of unusual halo phenomena. *Appl. Opt, 36,* 4195–4201.

Takano, Y., and K. Jayaweera, 1985: Scattering phase matrix for hexagonal ice crystals computed from ray optics. *Appl. Opt., 24,* 3254-3263.

Takano, Y., and K.N. Liou, 1989a: Solar radiative transfer in cirrus clouds. Part I. Single-scattering and optical properties of hexagonal ice crystals. *J. Atmos. Sci., 46,* 3-19.

Takano, Y., and Liou, K.N., 1989b: Radiative transfer in cirrus clouds. II. Theory and computation of multiple scattering in an anisotropic medium. *J. Atmos. Sci., 46,* 20-36.

Tompkins, A. M., K. Gierens, and G. Radel, 2007: Ice supersaturation in the ECMWF integrated forecast system. *Q. J. R. Meteorol. Soc., 133,* 53–63.

Travis, D. J., A. M. Carleton, and R. Lauritsen, 2002: Jet contrails and climate: anomalous increases in U.S. diurnal temperature range for September 11-14, 2001. *Nature, 418,* 601.

Waterman, P. C., 1971: Symmetry, unitarity, and geometry in electromagnetic scattering, *Phys. Rev., D3,* 825-839.

Weickmannn, H., 1945: Formen und Bildung atmosph¨arischer Eiskristalle. *Beitr. Phys. Atmos. 28,* 12–52.

Weickmann, H., 1949: Die Eisphase in der Atmosphäre. Ber. Dtsch. Wetterdienstes U.S.-Zone, 6, 3–54.

Wielicki, B. A., and L. Parker, 1992: On the determination of cloud cover from satellite sensors: The effect of sensor spatial resolution. *J. Geophys. Res., 97,* 12 799–12 823.

Wendling, P., R. Wendling, and H. K. Weickmann, 1979: Scattering of solar radiation by hexagonal ice crystals. Appl. Opt. 18, 2663–2671.

Yang, P., and K. N. Liou, 1995: Light scattering by hexagonal ice crystals: comparison of finite-difference time domain and geometric optics methods. *J. Opt. Soc. Amer. A,, 12,* 162-176.

Yang, P., and K. N. Liou, 1996a: Finite-difference time domain method for light scattering by small ice crystals in three-dimensional space. *J. Opt. Soc. Amer., A13,* 2072-2085

Yang, P., and K. N. Liou, 1996b: Geometric-optics-integral-equation method for light scattering by nonspherical ice crystals. *Appl. Opt., 35,* 6568-6584.

Yang, P., and K. N. Liou, 1997: Light scattering by hexagonal ice crystals: solution by a ray-by-ray integration algorithm. *J. Opt. Soc. Am. A., 14,* 2278-2288.

Yang, P., and K. N. Liou, 1998: Single-scattering properties of complex ice crystals in terrestrial atmosphere. *Contr. Atmos. Phys., 71,* 223-248.

Yang, P., K. N. Liou, K. Wyser, and D. Mitchell, 2000: Parameterization of the scattering and absorption properties of individual ice crystals. *J. Geophys. Res., 105,* 4699–4718.

Yang, P., H. Wei, H.-L. Huang, B. A. Baum, Y. X. Hu, G. W. Kattawar, M. I. Mishchenko, and Q. Fu, 2005: Scattering and absorption property database for nonspherical ice particles in the near- through far-infrared spectral region. *Appl. Opt., 44,* 5512–5523.

Yang, P. and K. N. Liou, 2006: Light Scattering and Absorption by Nonspherical Ice Crystals, in *Light Scattering Reviews: Single and Multiple Light Scattering,* Ed. A. Kokhanovsky, Springer-Praxis Publishing, Chichester, UK, 31-71.

Yee, S. K., 1966: Numerical solution of initial boundary value problems involving Maxwell's equations in isotropic media. *IEEE Trans. Antennas Propag., 14,* 302-307.

Yurkin, M. A., and A. G. Hoekstra, 2007: The discrete dipole approximation: an overview and recent developments, *J. Quant. Spectrosc. Radiat. Transfer,* doi:10.1016/j.jqsrt.2007.01.034.